Combustion and Flame 212 (2020) 142–155

Contents lists available at ScienceDirect

Combustion and Flame

journal homepage: www.elsevier.com/locate/combustflame

Comprehensive kinetic study of combustion technologies for low environmental impact: MILD and OXY-fuel combustion of methane

Ghobad Bagheri[a,b], Eliseo Ranzi[a], Matteo Pelucchi[a], Alessandro Parente[b], Alessio Frassoldati[a], Tiziano Faravelli[a,*]

[a] CRECK Modeling Lab, Department of Chemistry, Materials and Chemical Engineering "G.Natta", Politecnico di Milano, Piazza Leonardo da Vinci 32, 20133 Milano, Italy

[b] Aero-Thermo-Mechanics Laboratory, Ecole polytechnique de Bruxelles, Université Libre de Bruxelles, Avenue Franklin D. Roosevelt 50, CP 165/41, Brussels 1050, Belgium

ARTICLE INFO

Article history:
Received 11 April 2019
Revised 25 May 2019
Accepted 7 October 2019

Keywords:
MILD combustion
OXY-fuel combustion
Detailed kinetic mechanism
Methane

ABSTRACT

The development of processes with near-zero emissions such as MILD, flameless, and OXY-fuel combustion are of great interest in various energy scenarios. The assessment and design of new burners to meet energy demands and pollution reduction strongly depends on an accurate description of the chemistry involved in the combustion process. The main outcome of this study is the collection and review of a vast amount of experimental data on MILD and OXY-fuel combustion of methane that have been reported in recent years, together with a thorough kinetic analysis to identify aspects of the mechanism that requires further revision. The CRECK core model presented here is developed upon the Aramco 2.0 mechanism [1], and further extends the validation objectives to MILD and OXY fuel combustion conditions. The aim of this work is not only the mechanism validation but also a better understanding of the combustion characteristics and critical reaction pathways in MILD, flameless, and OXY-fuel combustion.

1. Introduction

The modern world depends heavily on energy generation in all its forms, and daily activities require a mix of thermal, mechanical and chemical energy. Determining the best energy source and generation technology is complicated. Even though the evaluation of alternative energy sources sometimes performed based on their economic sustainability and reliability in terms of production yields, the most controversial and essential criteria are the impacts of the various energy production technologies on public health and environment [2]. To further highlight the current interest in reducing the effects of energy production, the Paris Agreement [3] within the United Nations Framework Convention on Climate Change imposes new regulations to achieve carbon emission reduction.

Forecasting the global energy demand is extremely important for future energy policy and security. Considering various scenarios (New Policies, Current Policies, and Sustainable Development [4]) for energy production and demand, the role of natural gas will be significant, due to its environmental advantages and versatility relative to other combustible fuels. Natural gas is the cleanest fossil fuel emitting the lowest carbon dioxide per unit of energy. Despite its lower carbon density compared to other fossil fuels, its consumption demand is growing steadily by 1.6% in recent years, and its overall usage is expected to grow of 45% within 2040 [4].

The wide utilisation of natural gas for combustion applications emphasises the importance of understanding its combustion characteristics (methane, syngas (H_2/CO), and H_2/O_2 systems) in order to fulfil the goals in terms of energy efficiency and emission reduction. Moreover, a large part of our understanding of the complex combustion processes comes from elementary chemical kinetic models, and because of the hierarchical nature of combustion kinetics, the natural gas kinetic mechanism can be considered as the so-called "core chemistry" whose accuracy strongly influences heavier fuels combustion [5]. For this reason, the kinetic model development usually envisages a hierarchical extension from the core mechanism to heavier fuels, focusing mainly on the conventional combustion conditions of interest for engines and gas turbines. These conditions typically refer to pressures up to 100 atm and temperatures in the range of 500–2500 K, for different fuel/air dilutions.

Over the last decades, combustion studies have focused on the reduction of pollutant emissions, including NO_x, SO_x, CO_2,

* Corresponding author.
E-mail address: tiziano.faravelli@polimi.it (T. Faravelli).

https://doi.org/10.1016/j.combustflame.2019.10.014

CO, volatile organic components, and soot. Continuous advancements in control technologies have resulted in emission reduction and successfully demonstrated that efficiency improvements are the most attainable and cost-effective approaches. However, the long-term solution for decreasing combustion-generated pollution would require a larger reduction than that achieved only by efficiency improvements. For this reason, the development of industrial burners with Low or near-zero emissions such as those of interest for MILD (Moderate or Intense Low Oxygen Dilution) [6], FC (Flameless combustion) [7,8], HiTAC (High Temperature Air Combustion) [9], HiCOT (High Temperature Combustion Technology) [10], CDC (Colourless Distributed Combustion) [11], LTC (Low Temperature Combustion) [12], ULC (Ultra lean combustion) [13], and OXY-fuel combustion [14] has attracted a keen interest in energy policy.

According to Perpignan et al. [7], abbreviations such as flameless, HiTAC, MILD, HiCOT, and CDC refer to an analogous or slightly different regime but overlapping concepts; furthermore, acknowledged by Cavaliere and de Joannon [6] as a matter of terminology that could not be fully clarified. In view of the above consideration, combustion regimes such as HiTAC, HiCOT and CDC are usually attainable in different experimental/industrial facilities, where purely kinetic effects are not possible to decouple from fluid dynamics. MILD and OxyFuel combustion instead can be more easily investigated in simpler facilities (i.e. ideal reactors such as JSR and PFR), providing valuable experimental data for model development, validation and assessment as in the scope of this paper.

Both MILD and OXY-fuel combustion require a high dilution extent, which can influence the relative importance of chemical pathways. Despite the considerable potential of emission reduction of such technologies, inherent difficulties limit their extensive applications and successful integration at the industrial level. These inherent difficulties can be technical such as high-pressure loss [15], narrow operational conditions [16,17], fuel flexibility potentiality [7], and high CO emission [18–21], or a lack of fundamental understanding (limited experimental setup [22], almost no high-pressure experiments [7], turbulence–chemistry interaction and modelling issues [23], and complex diluent effects [24–26]) of MILD and OXY-fuel in a wide range of operating conditions. Furthermore, the predictive reliability of the kinetic models in these conditions has so far received a lower degree of attention compared to more conventional flame conditions. Thus, the primary goal of this work is to collect and review a vast amount of experimental data on MILD and OXY-fuel combustion and analyse them by using a detailed kinetic mechanism to identify aspects of the mechanism that require further revision. The aim is not only the mechanism validation but also that of highlighting hidden aspects and critical reaction pathways through a systematic discussion in the near-zero emission combustion processes (MILD and OXY-fuel).

This paper has been organised as follows. Section 2 briefly lays out the new combustion technologies, with a particular focus on MILD and OXY combustion processes. Then, Section 3 presents the general features of CRECK detailed kinetic mechanism. Sections 4 and 5 describe and discuss the broad set of experimental data from the available literature, which are useful not only for the validation of the mechanism but also to characterise and highlight peculiar aspects of these low environmental impact combustion technologies. Conclusions from the present analysis are reported in the last Section.

2. Low environmental impact combustions modes

Although the emission of sulphur and metal components depends strictly on fuel properties, CO, unburned hydrocarbons, NOx, polycyclic-aromatics, and soot particles can be reduced by adopting appropriate combustion technologies. High temperatures promote NOx formation, whereas low temperature does not guarantee complete combustion and CO and volatile components can be released. Moreover, incomplete mixing between fuel and oxygen at the molecular level occurring in diffusion flames causes rich local conditions thus favouring PAH and soot formation. For these reasons, new combustion technologies mainly move towards improved mixing, trying to reduce the maximum combustion temperature and turbulent fluctuations. In this direction, the Moderate or Intense Low oxygen Dilution (MILD) combustion is well recognized as an up-and-coming technique. MILD combustion takes place by preheating the reactants at a temperature higher than auto-ignition and by a very high dilution [27]. In fact, through the control of the maximum temperature employing flue gas recirculation and the extension of the reaction zone [28,29], it enhances combustion stability while remarkably reducing NOx emission.

Similarly, flameless combustion is defined as a regime in which two conditions must be satisfied:

(1) the reactant temperature must exceed self-ignition temperature;
(2) the reactants must entrain enough inert combustion products to reduce the final reaction temperature well below the adiabatic flame temperature, to such an extent that a flame front cannot be stabilised [8].

High-temperature air combustion (HiTAC) discussed by Hasegawa et al. [9] is an alternative technology mainly based on the preheating of air and control of the oxygen concentration in the reacting system. Another advantageous technique is the OXY-fuel combustion, which typically combines high purity oxygen (>95%) with recycled exhaust gases, always aiming to control the maximum flame temperature. Burning fuel in oxygen and flue gas rather than air, of course, results in the elimination of NOx emissions and also favours the carbon dioxide sequestration from the exhausts.

2.1. MILD combustion

The determination of the MILD regime confinement is still ambiguous, although numerous studies have been devoted to the classification and characterisation of its specific operating conditions. Studies in Jet Stirred Reactors (JSR) [30–32], Plug Flow Reactors (PFR) [27,33], jet-in-hot-coflow burners [34–36], and entrained flow jet flames [29,37,38] are only a small set of these examples. One well-known definition of MILD combustion is based on the initial temperature (T_{in}), the auto-ignition temperature (T_{Auto}), and the temperature increase during combustion (ΔT). A combustion regime is considered MILD if it satisfies the following conditions [6]:

$$T_{in} > T_{Auto} > \Delta T$$

MILD combustion is neither a diffusion flame nor a deflagration or detonation. It can be considered as a super diluted explosion or a continuous auto-ignition/explosion. The fluid-dynamic conditions and thermodynamic constraints under which MILD combustion develops are quite straightforward. There is no need of back-mixing for flame stabilisation, and the maximum temperature of the MILD Combustion processes is usually lower than 1600–1700 K. The mixing among fuel, oxidiser, and products streams are the crucial feature. The forced internal recirculation of the combustion products, which mix with the fresh mixture, supplies an adequate amount of enthalpy to reach the ignition temperature.

Although the auto-ignition temperature of the reacting system is the lowest temperature at which the system spontaneously ignites, the ignition propensity also depends on local oxygen and fuel concentrations, and it increases as the pressure or oxygen

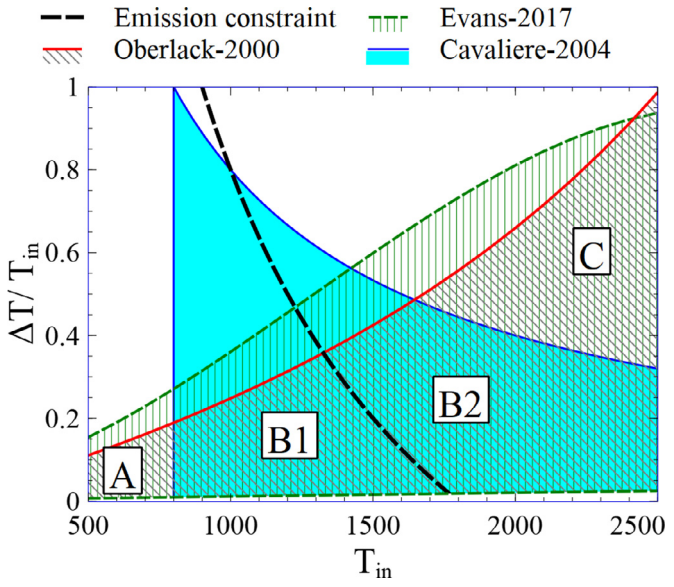

Fig. 1. Operative map of MILD combustion regimes. Region (A) Forced ignition, (B) MILD, and (C) HiTAC conditions (Cavaliere-2004 [6], Oberlack-2000 [10,39], and Evans-2017 [36].

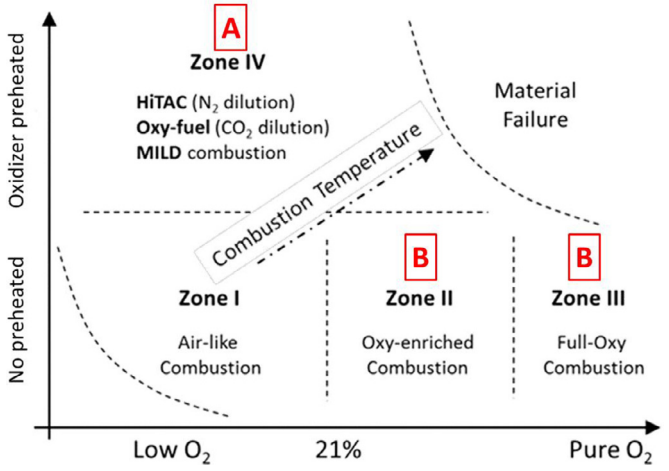

Fig. 2. OXY-fuel, HiTAC, and MILD combustion regimes as a function of the oxygen mole fraction and the preheat temperature of the reactants (after [47]). The regions denoted as A and B determine operating conditions of interest in the current research.

concentration increases. Therefore, the ideal MILD combustion requires a complete mixing at the molecular level, and the definition of T_{Auto} plays a vital role in the classification of MILD combustion.

A previous definition of the MILD combustion regime, without reference to the T_{Auto}, was initially proposed by Oberlack and Peters [10,39]. By assuming a single step irreversible reaction, constant thermochemical properties, and steady-state mass and heat conservation, the MILD combustion regime has to satisfy the following condition:

$$\frac{E_{Global}}{T_{in}R_u} < 4\left(1+\left(\frac{C_p W_f T_{in}}{QY_f}\right)\right)$$

Where E_{Global} is the effective activation energy of the global reaction, R_u the universal gas constant, C_p the constant pressure specific heat, Q the heat of combustion, W_f the fuel molecular weight, and Y_f the mass fraction of the fuel at the inlet. The term $(C_p W_f\ T_{in}/QY_f)$ is equivalent to $T_{in}/\Delta T$, indicating that MILD combustion requires the control of the temperature increase, ΔT.

Evans et al. [36] further discussed and extended this concept through the analysis of jet diffusion flames. The result obtained through counter-flow flamelet analysis provides a condition for the existence of ignition and extension turning points; therefore, the corresponding monotonic S-shape curve indicating MILD combustion is given by:

$$(\beta^2 + 6\beta + 1)\alpha^2 - (6\beta - 2)\alpha + 1 < 0$$

Where β is the activation temperature $(E_{Global}\ /R_u T_{st,b})$ and α refers to the heat release parameter $(\Delta T_{st}/T_{st,b})$ in stoichiometric and fully burnt conditions. These boundaries determine that the non-premixed MILD regime can take place with the increase of the initial temperatures, or the minimisation of the overall temperature increase and can be obtained following a forced ignition.

Figure 1 depicts the MILD combustion map according to the temperature definitions mentioned above [6,10,36,39], by assuming $T_{Auto} = 800$ K [40] and $E_{Global} = 40{,}000$ [cal/mol]. The intersection region (B1 and B2) satisfies the previous conditions, and it limits and defines MILD operative temperatures. Moreover, region (A) shows conventional combustion conditions, with an inlet temperature lower than T_{Auto}, thus requiring a forced ignition to propagate the flame [34]. Finally, the region (C) of the definition by Oberlack and Peters [10,36,39] allows higher temperature rises compared to the definition by Cavaliere and de Joannon [6]. According to these assumptions, ΔT may overcome 1300 K, when T_{in} is ~2000 K. It is clear that this high ΔT lowers the possibility of controlling the turbulent high-temperature fluctuations. Thus, this region can be classified as HiTAC, as it does not limit the temperature rise [9].

Due to the more uniform temperature distribution and limited peak temperature, MILD combustion strongly reduces the thermal NOx formation [41–43]. According to Zel'dovich mechanism, NOx formation rapidly increases at temperatures higher than ~1800 K, because of the high activation energy [44] of the rate-limiting reaction $O + N_2 = NO + N$ [6,45]. Thus, Fig. 1 also outlines an emission constraint (black dashed line) by limiting the maximum temperature to 1800 K. This line divides the MILD region into two zones of B1 and B2. The left-hand side (B1 or Clean-MILD) indicates the condition where air (N_2) is also a diluent. The presence of N_2 requires the maximum temperature limited to 1800 K (thermal NOx threshold) to reduce Nox formation. The right-hand side (B2 or Oxy-MILD) describes the zone where different diluent (CO_2, H_2O) allow higher operating temperatures.

2.2. OXY-fuel combustion

OXY-fuel combustion is one of the leading technologies and is of interest for CO_2 capture and storage in power generation plants. OXY-fuel is implemented by burning the fuel with nearly pure oxygen diluted with a large amount of recycled flue gas [46]. Various forms of OXY-fuel combustion have been used in different applications even before the concern over CO_2 sequestration raised in the world energy scenario. Figure 2 (adapted from Chen et al. [47]) schematises various OXY-fuel combustion conditions concerning the oxygen concentration and the preheating temperature of the reactants. Zone I of this figure is the so-called air combustion and the air-like OXY-fuel combustion zone, which involves a flue gas recirculation of ~ 60–80%. In this way, the oxidiser usually contains less than ~ 21% oxygen, and the flame temperature is lowered [47]. Zone II is the oxygen-enriched combustion area, where the oxygen concentration is significantly higher than 21%. Thus, the oxygen-enriched combustion features a higher sensible enthalpy and a higher flame temperature. Zone III is the full OXY-fuel combustion, where pure oxygen is used as the oxidiser. In this regime, the dilution is reduced to zero, and the pure oxygen highly intensifies the flame structure and the maximum temperature [48]. Finally,

zone IV depicts high-temperature OXY-fuel combustion and HiTAC that can be achieved by using highly preheated oxidiser. It should be noted that MILD combustion is also embedded in this zone where stable combustion is still attainable with oxygen mole fraction significantly lower than 21%.

Both Figs. 1 and 2 indicate the typical operating conditions of the new combustion technologies. Moreover, in Fig. 2, regions denoted as A and B determine operating conditions of interest in the current research. A and B cover both preheated and unpreheated oxidiser in a wide range of oxygen content (low content to pure oxygen). Temperatures and oxygen concentrations can vary in a wide range, and particular attention is required to analyse the effect of high levels of dilution, not only with N_2, but more importantly CO_2 and H_2O. Indeed, both water and carbon dioxide can have significant chemical effects, in addition to those related to their thermal properties. These features will be better analysed in Section 5, which discusses the collected set of experimental data at these conditions.

3. Kinetic model and numerical methods

The updated CRECK detailed kinetic mechanism has been used to analyse and discuss the experimental results. This kinetic scheme implements a C_0–C_3 core mechanism obtained by coupling the H_2/O_2 and C_1–C_2 from Metcalfe et al. [49], C_3 from Burke et al. [1] and heavier species from Ranzi et al. [50,51]. Several reactions, as listed in Table 1, are also updated for the sake of performance improvement. In the current mechanism, further enhancements were achieved by updating the acetaldehyde sub-mechanism, according to Pelucchi et al. [52].

Moreover, the rate rule for H-abstraction reactions of Ranzi et al. [53] was implemented and the rate parameters extracted in the absence of data from the literature (reference rate parameters can be found in Supplementary Materials). Indeed, the rate rule approach is more useful for the larger molecules. It is employed because the C_0–C_3 mechanism is not only a natural gas reaction mechanism but also a core mechanism for heavier fuel sub-mechanisms in CRECK kinetic scheme. Including H-abstraction rate rule facilitates linking this core mechanism to the remaining part of the mechanism.

The thermochemical properties of species were adopted from the most accurate databases in the literature. Hydrogen and Syngas cores were implemented from Active Thermochemical Tables (ATcT) [54]. Other important species thermochemical properties are extracted from Burcat's thermodynamic database [55]. For the rest of the species in the mechanism, which are not presented in databases, thermochemistry properties suggested in the CRECK mechanism [50] are used.

This model obtained from the above coupling was validated using the targets already presented in Metcalfe et al. [49], complemented by a vast database collected for this study. The kinetic model, with thermodynamic properties together with the complete validation supporting its reliability, can be found in the Supplementary Material of this paper. This version of CRECK kinetic mechanism, limited to methane, C_2, and light species, contains 114 species and 1941 reactions. Notably, there is a significant reduction in the number of species compared to the mentioned Aramco mechanisms.

The OpenSMOKE++ framework [66], developed at CRECK, was applied for the numerical simulations of reacting systems. This

Table 1
Modified reactions in the chemical kinetic model. The rate constants are in the form of $k = A\,T^n \exp(-E/(RT))$. Units are mol, cm, K, s, and cal.

Reactions	A	n	E_a	Reference
$C_2H_3+H=C_2H_2+H_2$	9.64E+13	0.0	0.0	[56]
C_3H_4-P+OH = $C_3H_3+H_2O$	2.00E+07	2.0	5000	[57]
C_3H_4-A+OH=$C_3H_3+H_2O$	2.00E+07	2.0	5000	[57]
$H+C_2H(+M) = C_2H_2(+M)$	1.00E+17	−1.0	0.0	[58]
$CH_3O+HCO=CH_3OH+CO$	1.00E+13	0.0	0.0	[56]
$H+O_2=O+OH$*	1.14E+14	0.0	15,286	[59]
$CH_3CO+O_2=CH_3CO_3$				
Logarithmic Pressure: 0.1	3.41E+69	−18.9	14,400	[60]
Logarithmic Pressure: 1.0	5.79E+61	−16.07	13,400	
Logarithmic Pressure: 10.0	5.07E+52	−12.96	11,560	
C_3H_4-P=C_3H_4-A				[61]
Logarithmic Pressure: 0.100	6.4E+61	−14.59	88,200	
Logarithmic Pressure: 1.000	5.2E+60	−13.93	91,100	
Logarithmic Pressure: 10.00	1.9E+57	−12.62	93,300	
Logarithmic Pressure: 100.0	1.4E+52	−10.86	95,400	
$CH_3+C_2H_6=CH_4+C_2H_5$	2.72E+00	3.767	9096	[62]
$H+C_3H_3 = C_3H_4$-A				
Logarithmic Pressure: 0.04	3.39E+36	−7.41	6337	[63,64]
Logarithmic Pressure: 1.00	3.16E+29	−5.00	4711	
Logarithmic Pressure: 10.0	8.71E+23	−3.20	3255	
Logarithmic Pressure: 100.0	2.05E+13	0.206	−173	
$H+C_3H_3 = C_3H_4$-P				
Logarithmic Pressure: 0.04	3.63E+36	−7.36	6039	[63,64]
Logarithmic Pressure: 1.00	7.94E+29	−5.06	4861	
Logarithmic Pressure: 10.0	1.07E+24	−3.15	3261	
Logarithmic Pressure: 100.0	6.40E+13	0.102	−31.2	
$H+C_3H_4$-$A=C_3H_5$-S				
Logarithmic Pressure: 0.04	3.38E+49	−12.75	14,072	[65]
Logarithmic Pressure: 1.00	1.37E+51	−12.55	15,428	
Logarithmic Pressure: 10.0	3.88E+50	−11.90	16,915	
Logarithmic Pressure: 100.0	2.17E+49	−11.10	18,746	
DUPLIICATE	2.98E+43	−11.43	8046	
Logarithmic Pressure: 0.04	5.75E+39	−9.51	7458	
Logarithmic Pressure: 1.00	4.33E+40	−9.60	6722	
Logarithmic Pressure: 10.0	3.44E+34	−7.36	6150	
Logarithmic Pressure: 100.0				

* Within the uncertainty the rate increased by 10%.

Table 2
List of experimental measurements studied in this paper.

Experiment	Mixture	Temperature [K]	φ	Pressure [atm]	Dilution	Reference
Jet stirred reactors	$1\%CH_4/O_2/N_2$	1000–1175	0.1	1	79%	[78]
	$1\%CH_4/O_2/20\%CO_2/N_2$	1000–1175	0.1	1	79%	[78]
	$1\%CH_4/O_2/10\%H_2O/N_2$	1000–1175	0.1	1	79%	[78,79]
	$CH_4/H_2/O_2/N_2(H_2 = 0–2\%)$	1025	0.3	1–10	90–92%	[80]
	$CH_4/H_2/O_2/20\%CO_2/N_2(H_2 = 0–2\%)$	1025	0.3	1–10	90–92%	[80]
Plug flow reactors	$CH_4/O_2/H_2O/N_2(H_2O = 0.35–9.3\%)$	1075–1800	1.6	1.1	98%	[81]
	$CH_4/O_2/85\%N_2$	1200–1400	0.1–0.8	1	85%	[27]
	$CH_4/O_2/85\%N_2$	1250	0.1–0.4	1	85%	[27]
	$CH_4/O_2/85\%N_2$	1300	0.1–0.7	1	85%	[27]
Laminar flame speeds	$CH_4/O_2(H_2O = 0–0.5)$	$T_{in} = 373$	0.5–1	1	0–50%	[82]
	$CH_4/O_2(CO_2 = 0–0.5)$	$T_{in} = 373$	0.5–1	1	0–50%	[82]
	CH_4 ($O_2/N_2 = 1/1$)(0–10%–20%H_2O)	$T_{in} = 373$	0.6–1.5	1	35–44%	[82]
	$CH_4/O_2/CO_2(XCO_2/(XCO_2+XO_2) = 0.4–0.7)$	$T_{in} = 300$	0.4–1.6	1–3	27–66%	[83]
Ignition delay times	$CH_4/O_2/30\%CO_2/AR$	1660–2000	1	0.76–3.77	89.5%	[84]
	$CH_4/O_2/30\%CO_2/AR$	1730–2000	0.5	0.77–3.92	91%	[84]
	$CH_4/O_2/CO_2/N_2(CO_2 = 0–75\%)$	1350–1900	0.5	1.75	75%	[85]

package can handle simulation of ideal chemical reactors (plug flow, batch, jet stirred reactors), shock tube and 1-D laminar flame. It also provides useful numerical tools such as the sensitivity and rate production analysis, which are applied to analyse and improve the whole kinetic mechanism.

4. Experimental dataset and mechanism validation

The different combustion regimes and dominant elementary chemical pathways of fuel oxidation depend on operating temperatures and pressures [67]. Compared to flame combustion conditions, MILD combustion lowers the operating temperatures, while the radical pool and the OH concentration is more homogeneously distributed in the reaction zone [22,68]. Although MILD combustion has been widely investigated [6,26,27,69–71], only minor attention has been devoted to the validation of detailed kinetic mechanisms in these conditions, mostly underlining shortcomings of existing kinetic models.

Hierarchically, the pyrolysis and combustion of methane are interconnected to the oxidation of any hydrocarbon fuels. Mainly the competition between the oxidation of methyl and recombination paths to form C_2 species plays a crucial role in reactivity. Recent studies of de Joannon and co-workers [33,71,72] highlighted the importance of the core kinetics (C_0–C_2) in MILD combustion of fuels other than methane. Methyl recombination reactions forming ethane and successive dehydrogenation leading to ethylene and acetylene are important in PAHs and soot formation [73]. The motivations above highlight the criticism involved in the validation of methane sub-mechanism, as its chemistry strongly influences other systems of interest (i.e. heavier fuels and pollutant formation) [74,75].

At low temperatures, methane is more stable compared to other hydrocarbons, due to the lack of C–C bonds and the only presence of stronger aliphatic C–H bonds. Thus, methane thermal decomposition is highly endothermic and requires ~105 kcal/mol energy for breaking the C–H bond. Moreover, there are fundamental difficulties associated with the high-temperature pyrolytic conditions because of the formation of PAHs and soot [76,77]. Thus, compared to oxidation experiments, the experimental data on methane pyrolysis are scarce and are mainly limited to low and atmospheric pressures to prevent or limit carbon formation. Therefore, the development and validation of the kinetic mechanisms are based only on these limited number of experimental observations. As already discussed in the literature [75], the detailed kinetic mechanism of methane pyrolysis and oxidation limited to C_1 and C_2 species can present discrepancies in H_2 and C_2H_2 formation, because of the possible growth of PAH and unsaturated species. In order to guarantee the model accuracy at very rich pyrolytic conditions, the heavier species and their successive reactions to form butadiene, PAH and aromatic species need to be accounted for.

At fixed fuel concentration, methane reactivity increases as the equivalence ratio decreases. In fact, oxidation channels with the formation of formaldehyde prevail over pyrolysis channels in lean fuel mixtures, whereas, in rich conditions, the reactivity decreases because of the pyrolytic pathways favoured by the recombination of methyl radicals and the successive dehydrogenation steps. Moreover, pyrolysis is an endothermic process, thus decreasing the reactivity not only by forming more stable radicals but also through temperature reduction [78].

Although the extended and complete set of experimental conditions and their validations are reported in the Supplementary Material, Table 2 summarises the conditions of a selected set of experimental data useful for the validation of methane oxidation mechanism and to extended the knowledge of diluted combustions by means of a broad set of comparison of experimental data, model simulations and kinetic analyses. These experiments of MILD and OXY-fuel combustion are divided into four different categories including jet-stirred reactor (JSR), plug flow reactor (PFR), flame speeds and ignition delay times. For the complete validation of the CRECK kinetic mechanism, readers can refer to the Supplementary Material.

Notably, the following aspects of MILD and OXY-fuel combustion and the effect of CO_2 and H_2O dilution will be analysed and discussed:

- System reactivity in ideal reactors.
- Laminar flame speed (oxy-fuel systems).
- The ignition delay time in shock tubes and plug flow reactors.
- Thermo-chemical oscillation in Jet stirred reactors.

5. Model validation and discussion on the effect of CO_2 and H_2O

5.1. System reactivity in ideal reactors

Based on different experimental data, this section analyses sequentially the effect of CO_2 and H_2O dilution in lean methane mixtures [78,79], then the effect of CO_2 dilution in a lean CH_4/H_2 system [80], and finally, the effect of H_2O addition in rich methane mixtures at high-temperatures [81].

5.1.1. CO_2 and H_2O dilution in lean methane mixtures

Figure 3 shows methane oxidation profiles in three different diluted mixtures N_2, (N_2+20% CO_2) and (N_2+10% H_2O) versus the reactor temperature. Ultra-lean fuel mixtures (φ = 0.1) were

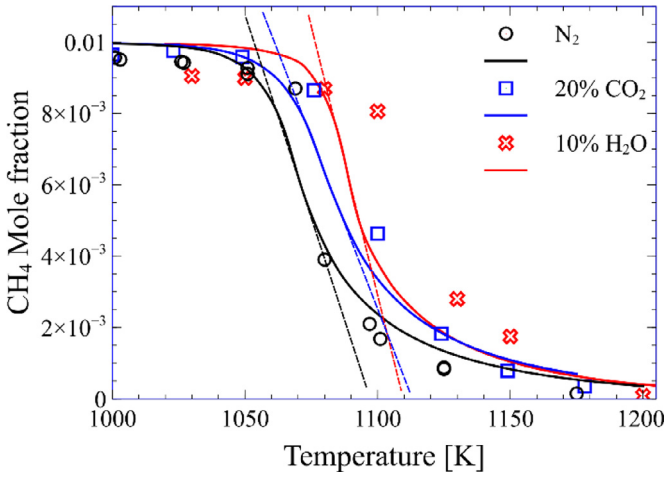

Fig. 3. Methane concentration profiles vs temperature in three diluted systems at atmospheric pressure and ultra-lean conditions ($\varphi = 0.1$). Reactants are diluted with 79% N_2, (59% N_2+20% CO_2), and (69% N_2+10%H_2O). Symbols: experimental data [78,79], lines: results from kinetic model simulations.

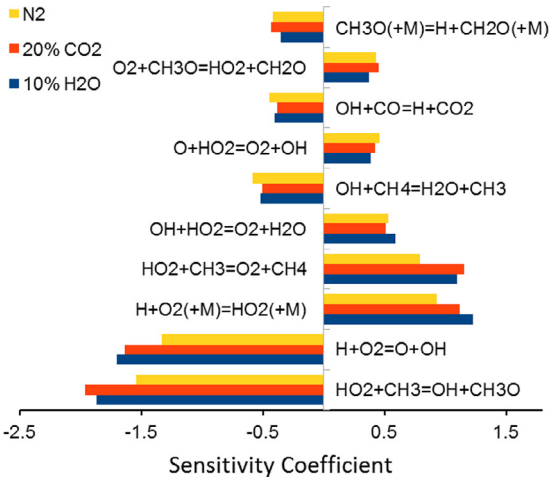

Fig. 4. Sensitivity analysis of CH_4 concentration in the three diluted systems presented in Fig. 3 at $T = 1100$ [K].

experimentally studied in a JSR at atmospheric pressure and steady-state conditions [78,79]. High dilution and preheating before injection minimised temperature gradients inside the reactor, accordingly, near isothermal conditions were obtained. It is evident that CO_2 and H_2O dilutions cause a delay in the system reactivity, which slightly shifts CH_4 conversion toward higher temperatures, compared to the N_2 diluted system. Simulations reasonably agree with experimental data even if the dilution effect is underestimated, mainly in the H_2O diluted system. At temperatures higher than 1200 K, all the systems converge toward a complete CH_4 conversion. Comparing the dashed lines of Fig. 3, one can first observe a temperature delay of about 10–20 K, when adding CO_2 or H_2O, respectively. Moreover, it is possible to observe that, after a delay in CH_4 conversion, the H_2O diluted system shows a higher increase of reactivity with respect to the other systems.

In these isothermal conditions, the CO_2 and H_2O dilution change the system reactivity, because of chemical reactions and/or collisional efficiencies. It is noteworthy that the competition between the two pathways of $H + O_2$ (R1 and R2) plays a crucial role in defining the system reactivity in this intermediate temperature range.

$$H + O_2 = O + OH \quad (R1)$$

$$H + O_2 + M = HO_2 + M \quad (R2)$$

The chain branching reaction (R1) is the key step in all combustion systems, clearly emerging in sensitivity plots for all fuels under high-temperature conditions (T>1000 K) [86]. Any active channel that competes with (R1) and reduces H radical concentration results in diminishing overall oxidation rate [50]. The kinetic interaction involving radical chain branching (R1) coupled with the inhibition or HO_2 stabilisation (R2) caused by the third-body efficiency of bath gases can affect the k_1/k_2 branching ratio.

In the view of the above considerations, the third-body efficiencies effects can explain the different delays in the start of methane conversion in Fig. 3, as the third-body efficiency of H_2O and CO_2 in reaction (R2) are 10 and 3.8, respectively [49]. By merely considering the mole fraction of the bath gases as presentative of their concentrations and also accounting for their collisional efficiencies, the following order of delay in reactivity (τ_i) as a function of temperature is justified:

$$\tau_{N_2} < \tau_{N_2+CO_2} < \tau_{N_2+H_2O}$$

This fact is well confirmed by the sensitivity analysis shown in Fig. 4, where the sensitivity coefficient of reaction (R2) is the highest in the water-diluted system and the lowest in the N_2 system. This dependence on the third body is particularly important in modelling of OXY-fuel [87], MILD [6], and exhaust gas recirculation (EGR) [88,89] systems, where the mole fractions of multiple colliders other than N_2 are increased.

It is noteworthy to mention that the abundant availability of HO_2 from (R2) also increases the importance of the competition between recombination and dismutation channels of CH_3 and HO_2 radicals (R3 and R4).

$$HO_2 + CH_3 = OH + CH_3O \quad (R3)$$

$$HO_2 + CH_3 = O_2 + CH_4 \quad (R4)$$

While the termination reaction to form CH_4 and O_2 (R4) reduces the system reactivity and methane conversion (positive sensitivity coefficient), the propagation reaction (R3) to form the two reactive radicals CH_3O and OH evidently increases methane conversion (negative coefficient). As shown in Fig. 4, the system reactivity is dominated by the chain branching reaction (R1), and the ignition happens when it prevails over (R2). (R1) enhances the concentration of O and OH radicals, which will, in turn, further enhance OH production via reaction (R5), particularly in the diluted water system.

$$O + H_2O = OH + OH \quad (R5)$$

5.1.2. CO_2 dilution in a lean CH_4/H_2 combustion system

Cong and Dagaut [80] likewise investigated the effect of hydrogen addition to the oxidation of methane in a JSR at different pressures (1 and 10 atm) first with neat N_2 dilution, then with a 20% CO_2 addition. Together with the fuel (CH_4 /H_2), a fixed amount of O_2 (6.67% mol) was fed to the system at a constant equivalence ratio of 0.3. As expected, their results confirmed that H_2 addition promotes methane conversion. Indeed, the hydrogen addition enhances H and OH radical concentrations, through the H_2–O_2 sub-mechanism. At lean conditions, hydrogen promotes H radical concentration through the H abstraction reactions by OH and O radicals, more effectively than CH_3 radicals.

$$H_2 + O = OH + H \quad (R6)$$

$$H_2 + OH = H_2O + H \quad (R7)$$

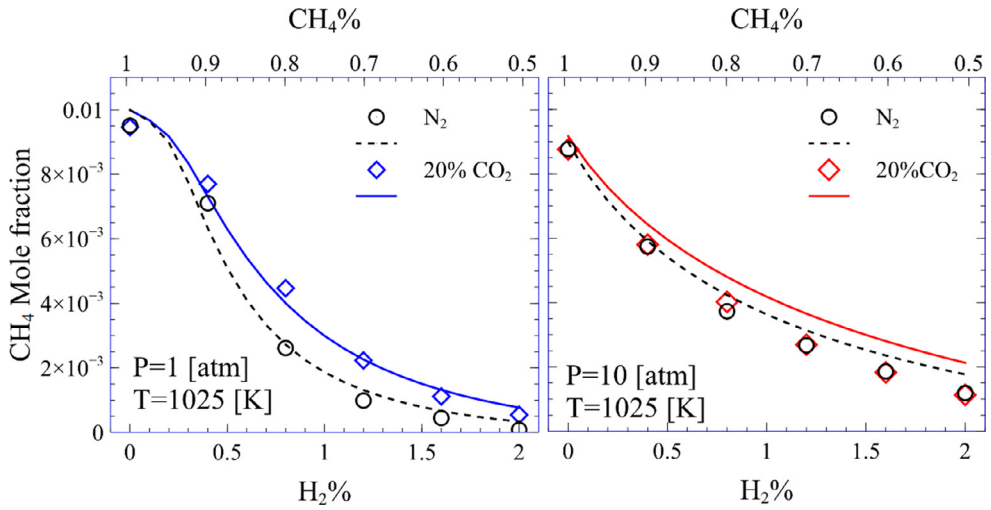

Fig. 5. Effect of H_2 addition on CH_4 conversion in a JSR at 1 and 10 atm, with and without 20% CO_2 addition. Conditions: 6.67% oxygen, $\varphi = 0.3$, $T = 1025$ K. Symbols: experimental data [80], lines: results from kinetic model simulations.

Higher H concentrations, in turn, increase OH radical formation via (R1) and (R8) reactions.

$$HO_2 + H = OH + OH \quad (R8)$$

In contrast, 20% CO_2 addition partially reduces the reactivity because of the higher collision efficiency in (R2). Figure 5 shows the satisfactory comparison of experimental data and model predictions at constant temperature ($T = 1025$ K) at two different pressures (1 and 10 atm), both for the neat N_2 and the 20% CO_2 cases. Due to the pressure dependence of the unimolecular CH_4 decomposition reaction, there is a small conversion (5%) of pure CH_4 at 10 atm, whereas it does not show any reactivity at atmospheric pressure. Hydrogen addition favours methane oxidation by promoting H radical formation, and this effect is more evident at atmospheric pressure. When comparing the methane concentrations profiles versus H_2 additions at 1 and 10 atm, it is possible to highlight a different behaviour. There is an initial higher reactivity at higher pressure, but only with low hydrogen additions. At atmospheric pressure, after a small induction, H_2 additions favour a higher reactivity, and the system becomes more reactive, after 1–1.3% H_2.

Figure 6 presents the sensitivity analysis of methane reactivity for the cases shown in Fig. 5 with 1% hydrogen. The different sensitivity coefficients of reactions (R1) and (R2) highlight that their competition is more effective at 1 atm, and mainly in the N_2 diluted systems. The CO_2 addition, as well as the higher pressure favour the HO_2 formation, and this competition becomes less effective. Thus, the CO_2 diluted system at 10 atm shows the lowest sensitivity coefficients to both reactions.

As the HO_2 formation is preferential at higher pressure, the competition between two chain propagation (R3) and termination (R4) reactions, becomes more important despite a decrease of sensitivity coefficient in terms of absolute values. A complete mechanism validation and analysis of these experimental data of Cong and Dagaut [80] on the effect of hydrogen additions on methane conversion is presented in the Supplementary Materials.

5.1.3. H_2O addition in rich methane mixtures at high-temperatures

Rasmussen et al. [81] studied the effect of H_2O addition on CH_4 oxidation at rich conditions ($\varphi = 1.6$) in an isothermal plug flow reactor at high temperatures (1073–1823 K), and atmospheric pressure. To further improve the assessment, five cases with different water additions (from 0.35% to 9.28%) are selected. Figure 7 confirms that the kinetic mechanism is able to capture CH_4 conversion profiles versus temperature with different extent of water addition. This effect on CH_4 reactivity is indeed quite marginal at these high-temperature conditions, where a possible increase of the reactive flux $H + O_2 \leftrightarrow HO_2 \leftrightarrow H_2O_2$ formation (because of R2) cannot influence the system reactivity as H_2O_2 is rapidly decomposed to OH radicals.

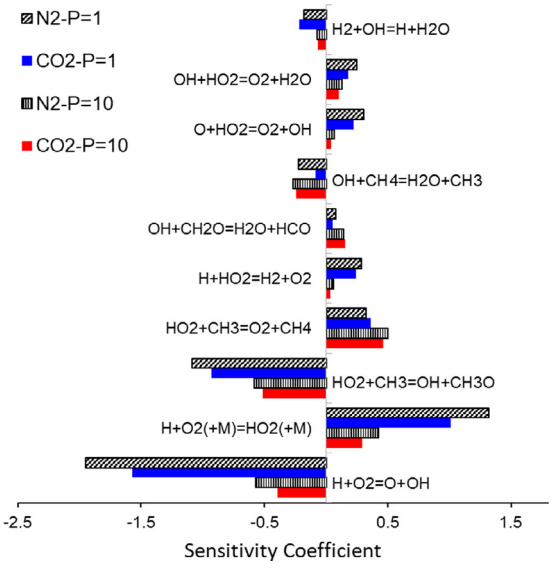

Fig. 6. Sensitivity analysis of methane concentrations for the four cases presented in Fig. 5. CH_4 doped with 1% H_2, at 1025 K and $\varphi = 0.3$.

Although methane conversion profiles are similar, the CO_2 formation is affected by H_2O addition. In particular, Fig. 7 shows that CO_2 formation grows with increasing water dilution. The water-gas shift process ($CO+H_2O=CO_2+H_2$) explains this behaviour. Indeed, the increased concentration of OH radical further supports reaction(R9).

$$CO + OH = CO_2 + H \quad (R9)$$

As highlighted by Rasmussen et al. [81], the H_2O addition favours OH and H_2 formation and also inhibits soot formation owing to its chemical effects on the oxidation of C_2H_2 preventing from further molecular growth at T>1500 K. Promoting OH and H_2 formation from H_2O justifies the changes in C_2H_2 chemistry, which

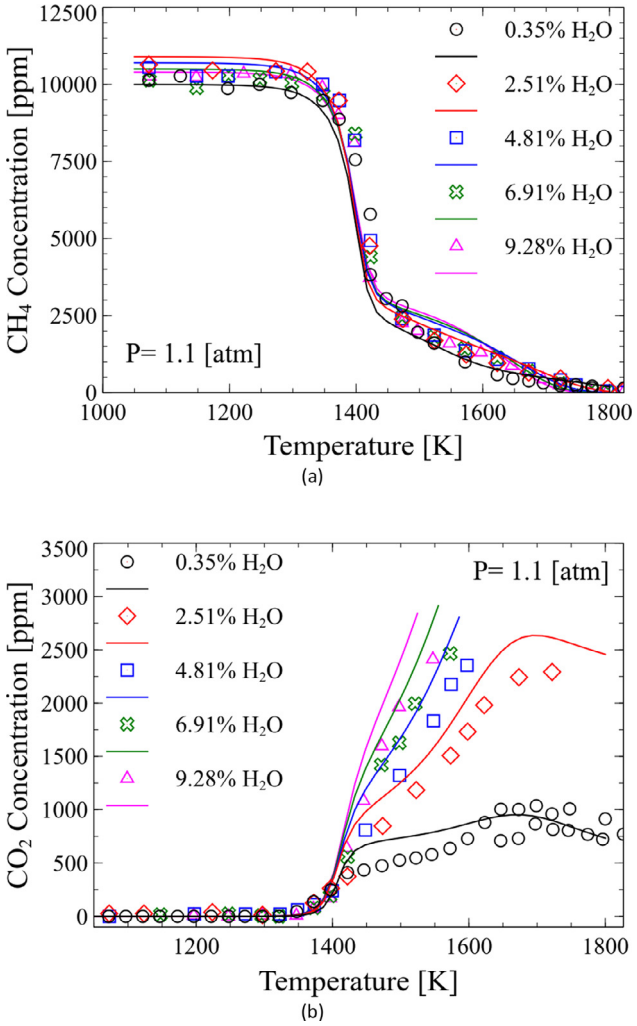

Fig. 7. Comparison of methane and CO_2 profiles between experimental data (points) and model simulations (lines) in a PFR for five H_2O diluted systems. Conditions: $P = 1.1$, $\varphi = 1.6$, and $CH_4/O_2/N_2$ diluted with 0.35, 2.5, 4.8, 6.9, 9.3% H_2O. Experiments refer to [81].

reduces or eliminates soot formation in temperatures higher than 1500 K.

5.2. Laminar flame speed (OXY-fuel systems)

Laminar flame speed is one of the most critical combustion properties of a fuel. It is a function of the thermodynamic state of the fuel/oxidiser mixture (pressure, temperature, and composition). The mixture composition defines the net fundamental properties effects on diffusivity, reactivity, and exothermicity [50].

Thus, CO_2 and H_2O dilution can change the system reactivity not only because of chemical effects but also due to their different physical properties. Indeed, the physical effect of the diluent occurs by altering heat capacity, transport properties, and thermal diffusion of the reacting system, whereas the chemical effect is the result of the intrinsic reactivity of CO_2 and H_2O in the system. In order to distinguish between chemical and physical effects on system reactivity, it can be convenient to assess the extent of the two competing effects in CO_2 and H_2O diluted systems by using dummy inert species (CO_2^* and H_2O^*) with the same thermal properties of the real species (CO_2 or H_2O), but not involved in the reaction mechanism [78,90].

The effect of H_2O and CO_2 addition on premixed flames at OXY-fuel conditions was systematically investigated by Mazas et al. [82].

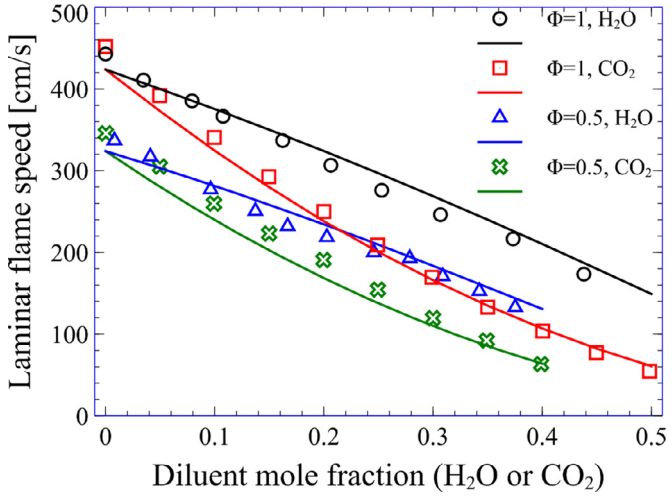

Fig. 8. Laminar flame speed of $CH_4/O_2/H_2O$ and $CH_4/O_2/CO_2$ mixtures, for $\varphi = 0.5$ and $\varphi = 1$ at $T_{in} = 373$ K and atmospheric pressure. Symbols refer to experimental data [82] and lines to model predictions.

They examined the effect of the oxygen enrichment ratio, equivalence ratio, and H_2O addition on N_2 and CO_2 diluted mixtures. Mazas et al. [82] highlighted a quasi-linear decrease in the laminar flame speed of $CH_4/O_2/N_2/H_2O$ and $CH_4/O_2/CO_2/H_2O$ by increasing the water addition. These experimental data are useful for mechanism evaluation at high flame temperatures. A selected set of data from Mazas et al. [82] will be discussed in this section; additional comparisons can be found in the Supplementary Materials.

The first set of experiments in Fig. 8, compares the experimental and predicted effect of H_2O and CO_2 dilution in full OXY-fuel combustion (CH_4/O_2) for lean ($\varphi = 0.5$) and stoichiometric ($\varphi = 1$) mixtures. It is evident from this figure that CO_2 has a more discernible effect on laminar flame speed reduction comparing to H_2O. The more substantial effect of CO_2 dilution is well captured by the model and is mainly due to the lower flame temperature, because of the higher heat capacity of CO_2. As thermochemical properties of CO_2 and H_2O are different from those of N_2, and their involvement in the reaction system changes the flame temperature, the laminar flame speed, and other characteristics of high-temperature combustion.

Mazas et al. [82] also reported experimental data of premixed laminar flame speeds of $CH_4/O_2/N_2/H_2O$ systems with three different H_2O addition ($X_{H_2O} = 0.0, 0.1 \text{and} 0.2$)in the range of equivalence ratio 0.6–1.6.

Figure 9(a) shows a good agreement between model predictions and experimental data. The water addition reduces the flame speed over the entire equivalence ratio range. Dashed lines in Fig. 9(a) indicate the predictions obtained by using the dummy species (H_2O^*) to distinguish the physical from the chemical effects. The superimposed profiles highlight that the physical effects of water are here prevailing over a very weak chemical effect.

Despite the minimal chemical effect, Fig. 9(b) provides the sensitivity analysis of the laminar flame speed at $\varphi = 1$ for the various H_2O dilutions. As discussed by Ranzi et al. [50], the chain branching reaction (R1) is the key step in all the combustion systems and any active channel that competes with (R1) and reduces H radical concentration results in diminishing overall oxidation rate. Namely, the third body reactions (R2) and (R10) directly compete with reaction (R1), inhibiting the reactivity, and suppressing the flame speed.

$$H + CH_3 + M = CH_4 + M \qquad (R10)$$

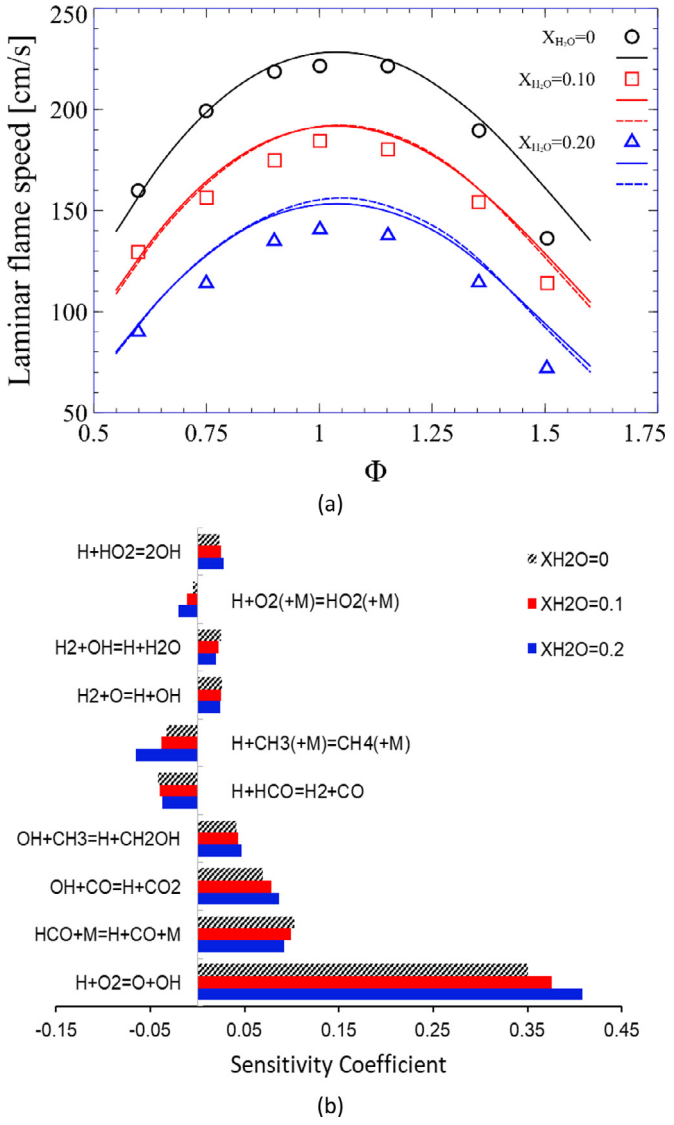

Fig. 9. (a) Enriched laminar flame speed of CH_4 ($O_2/N_2 = 1$) diluted with 0, 10 and 20% H_2O at $T_{in} = 373$ K and atmospheric pressure. Symbols refer to experimental data [82], solid and dashed lines refer to model predictions with H_2O and dummy H_2O^*, respectively. (b) Sensitivity analysis of the laminar flame speed at the stoichiometric condition.

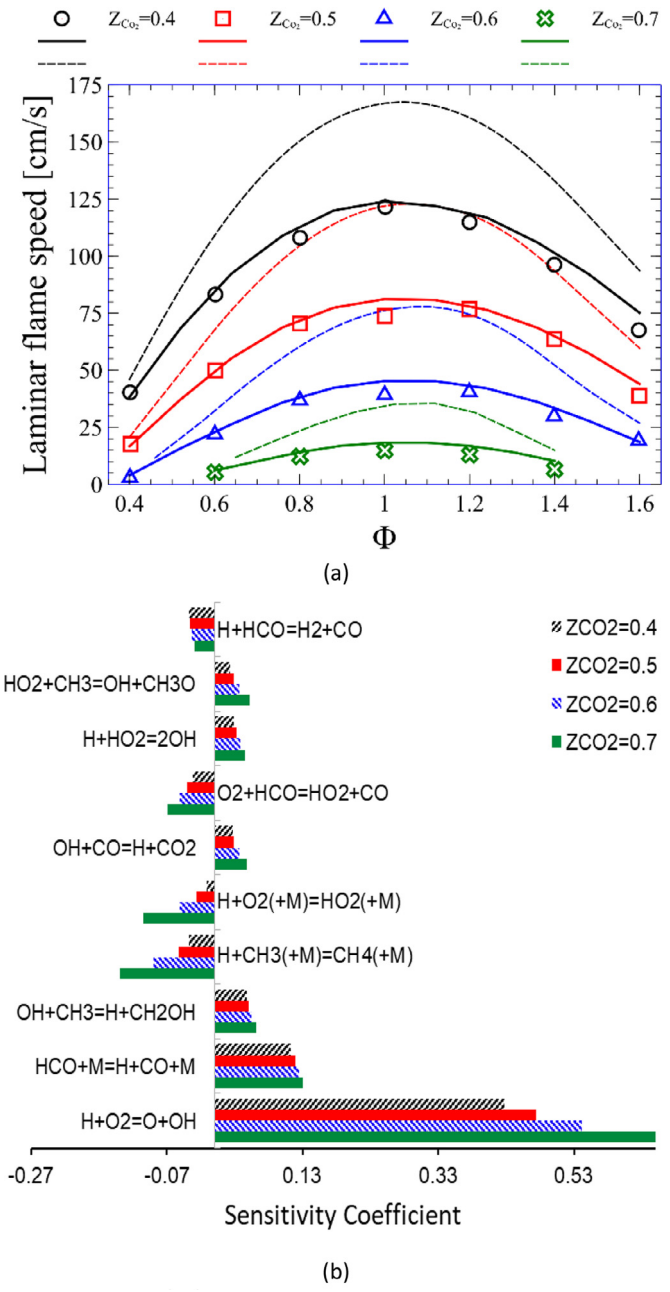

Fig. 10. (a) Laminar flame speed of $CH_4/O_2/CO_2$ mixtures at $T_{in} = 300$ K and atmospheric pressure. CO_2 mole fraction is defined by $Z_{CO_2} = X_{CO_2}/(X_{CO_2} + X_{O_2})$ Symbols refer to experimental data [83], solid and dashed lines are model predictions with reactive and unreactive CO_2. (b) Sensitivity analysis on the laminar flame speed of the different cases of the panel (a) at $\Phi = 1$.

This recombination reaction works as radical sink affecting flame speed and the ignition delay time of practically all the hydrocarbon and oxygenated fuels. As mentioned in the discussion of Fig. 3, a higher H_2O collision efficiency slightly reduces the model deviations as water addition increases. Reactions (R2) and (R10) have been widely studied, both experimentally and theoretically; however, uncertainties still exist in the first principle assessment of collisional efficiencies [91–94].

Recently, laminar flame characteristics of methane OXY-fuel combustion highly diluted with CO_2 were experimentally analysed by Xie et al. [83] in a constant volume chamber. They measured the laminar flame speed of various CO_2 diluted systems at three different pressures (1, 2 and 3 [atm]). Figure 10(a) satisfactorily compares experimental data with model predictions and highlights the strong effect of CO_2 additions. The dashed lines show the predictions obtained by using the dummy species (CO_2^*). Although the physical effect of CO_2 dilution results in a substantial reduction of the flame temperature, it is relevant to observe that there is also a critical inhibiting effect of CO_2, mainly in stoichiometric conditions, due to the reaction (R9).

To better assess the effect of CO_2 dilution on the flame speed, Fig. 10(b) presents the sensitivity analysis to laminar flame speed for the four different dilutions at $\varphi = 1.0$. Similar to the previous analysis, the chain branching reaction (R1) has the highest sensitivity coefficient, and CO_2 addition further increases its importance. The sensitivity coefficients of third body reactions (R2 and R10), at different CO_2 dilutions, shows the increasing importance of these reactions in the reduction of the flame speed. Higher third body efficiency of the (R2) favours HO_2 formation and the propagation reactions:

$$H + HO_2 = OH + OH \quad (R11)$$

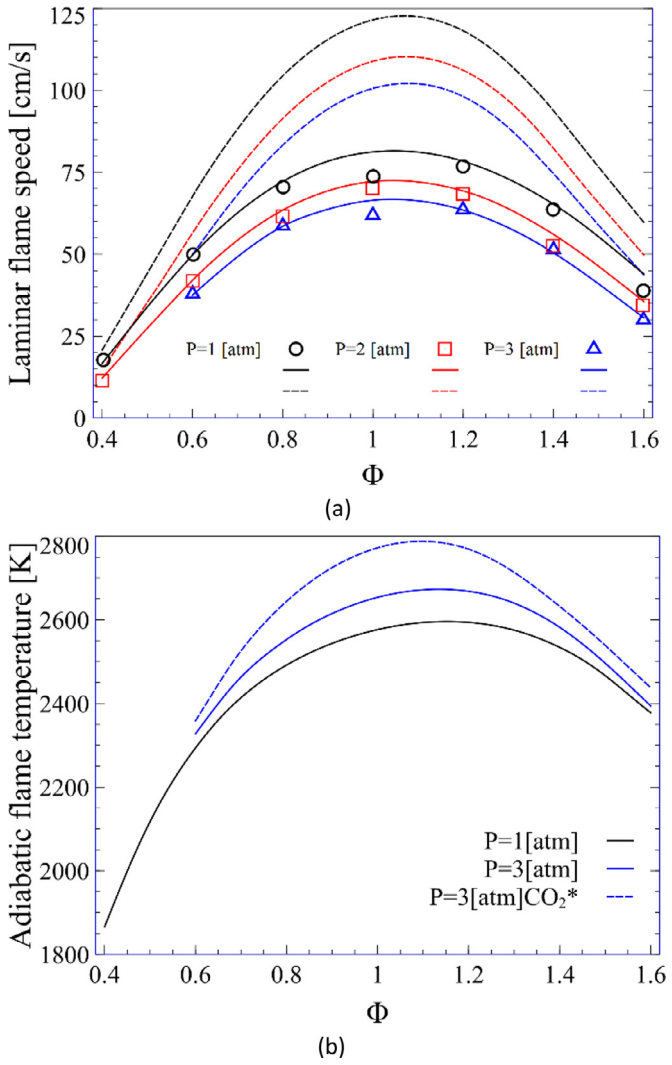

Fig. 11. (a) Laminar flame speed of $CH_4/O_2/CO_2$ mixtures at 1,2 and 3 atm and T_{in} = 300 K. CO_2 mole fraction is defined by $ZCO_2 = XCO_2/(XCO_2+XO_2)$. Symbols refer to experimental data [31], solid and dashed lines are model predictions with reactive and unreactive CO_2*. (b) Adiabatic flame temperatures at 1 and 3 atm. Lines are model predictions with reactive (solid) and unreactive CO_2 (dashed).

$$CH_3 + HO_2 = CH_3O + OH \quad \text{(R12)}$$

become more sensitive at higher CO_2 dilution.

As a final example of the chemical effect of CO_2 dilution on the laminar flame speed, a $CH_4/O_2/CO_2$ system is analysed in the whole range of equivalence ratios, at different pressures (1, 2 and 3 atm) and T_{in} = 300 K. The CO_2 fraction inside the $CH_4/O_2/CO_2$ mixture Z_{CO_2}, defined as $X_{CO_2}/(X_{CO_2}+X_{O_2})$, is equal to 0.5. Figure 11(a) presents the comparison between experimental measurements of laminar flame speeds [83] and model predictions. Solid and dashed lines indicate the model predictions with reactive CO_2 and unreactive CO_2* dilution, respectively. At higher pressures, the flame speed diminishes, mainly because of more substantial influence of the third body recombination reactions. Figure 11(b) presents the predicted adiabatic flame temperature at 1 and 3 atm. As expected, because of the lower importance of the endothermic dissociation reactions, the adiabatic flame temperature increases, when pressure increases. Correspondingly, despite the decrement in laminar flame speed at higher pressures, the burning velocity of the mixture increases [50]. Moreover, from Fig. 11(b) it is possible to see a significant temperature rise when working with the unreactive (CO_2*) dilution. Besides the considerable importance of recombination reactions, model predictions indeed show that CO_2 dilution globally promotes the endothermic reverse of the water gas shift process:

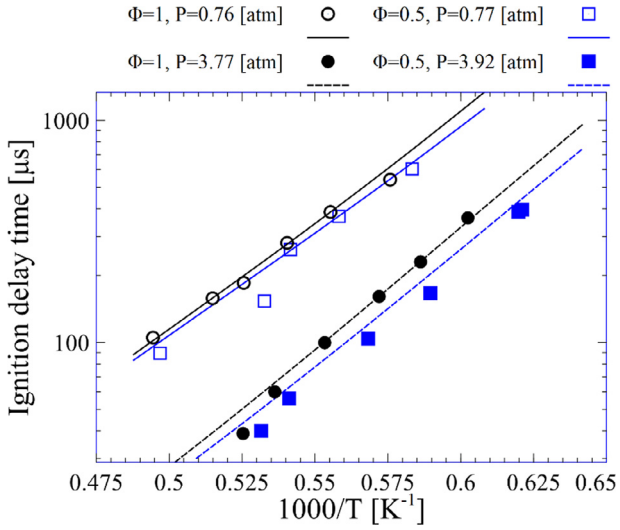

Fig. 12. Comparison of ignition delay times at two different pressure, 0.77 and 3.85 and stoichiometric and lean mixtures (0.5) diluted with 30% CO_2. Symbols: experimental data [84], lines: results from kinetic model simulations.

$$CO + H_2O = CO_2 + H_2 \quad \text{(R13)}$$

This feature additionally reveals the explanation of the predicted higher flame temperatures within the unreactive (CO_2*) dilution.

5.3. Ignition delay time

Optimal operating conditions to design industrial burners and devices require a thorough assessment of chemical time scales (typically the ignition delay time) and auto-ignition temperatures. Thus, industrial applications of new combustion technologies ask for the identification of optimal operating conditions to obtain high efficiency and to lower pollutant emissions. The ignition delay time is an intrinsic characteristic ruled by fuel chemistry, driving the assessment of optimal operating conditions and the definition of critical parameters such as the times scales needed to establish combustion within the mixing layer or the length limitation in combustor design [95].

5.3.1. OXY-fuel ignition delay time in shock tube reactors

Exhaust gas recirculation (EGR) in OXY-fuel combustion involves a large amount of CO_2 and H_2O. Thus, as said, it strongly modifies the reacting system regarding kinetic and thermal effects. Shock tubes may encounter many flows field non-idealities in the presence of polyatomic molecules (CO_2 and H_2O); however, this behaviour is not exclusive to specific bath gases, and different gases can similarly cause bifurcation in shock tubes [85]. As a result, a limited number of shock tube studies considering CO_2 as bath gas can be found in the literature [84,85,96–98].

Figure 12 shows the ignition delay times of different $CH_4/O_2/CO_2$ mixtures (φ = 0.5 and 1) at 1 and 4 atm measured in a shock tube [84]. Mixtures are diluted with 30% CO_2. At a given pressure, the ignition delay times of the lean mixtures are shorter than those of stoichiometric concentrations. The pressure rise shortens the ignition time by a factor of ~3–5; furthermore, this behaviour is also more noticeable at lower temperatures. The difference between the lean and the stoichiometric mixture

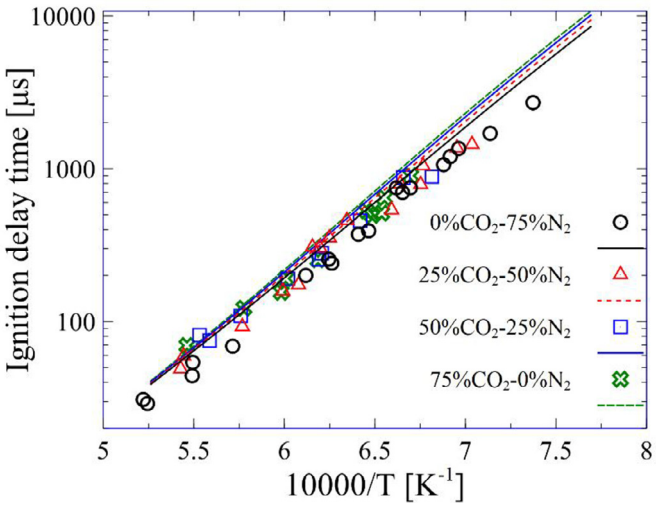

Fig. 13. Ignition delay times for a lean mixture ($\varphi = 0.5$) in various CO_2 dilution levels at 1.75 atm. Experimental data refers to [85].

increases from ~10% to ~20% moving to higher pressures. The kinetic mechanism accurately captures both these trends, as well as the variations of the apparent activation energy of these data. In fact, by raising the pressure from 0.77 to 3.85 atm, the apparent activation energy moves from 52,000 cal/mol to 47,000 cal/mol, with limited dependence on the stoichiometry.

Hargis et al. [85] performed experimental measurements of methane ignition delay in the presence of CO_2 in a shock tube. Fig. 13 compares experimental ignition delay times with model predictions alongside with the effect of CO_2 addition (0, 25, 50, 75%), at 1.75 atm. These results demonstrate that the CO_2 dilution plays only a negligible role in the ignition delay times, under the investigated conditions. Moreover, the differences in the ignition delay time of all the mixtures seem very marginal, within the uncertainty of the measurement. This similarity in the ignition delay times highlights that CO_2 is scarcely reactive during the ignition, because of its stability, and does not actively modify the pool of radical. In contrast, a minimal increase in predicted ignition delay times can be observed at low temperatures. These small variations seem to indicate a limited effect of the third-body efficiency of CO_2 on the ignition mechanism. In this regard, it is essential to underline that the collisional efficiencies of different colliders are not well characterised, and they are often treated empirically as the dependency of the collisional energy transfer on temperature, bath gas, and chemical structure of reactant are not fully understood. Jasper et al. [93] extended a theoretical characterisation of the collisional energy transfer in master equation simulations of methane dissociation for combustion applications. They pointed out that collision efficiencies can vary with the temperature; however, the trend of these variations depends on the chemical structure of bath gases. This temperature dependence is stronger for lighter bath gases (He and H_2), while polyatomic gases have the weakest temperature dependence (H_2O and CH_4).

5.3.2. MILD combustion in plug flow reactors

Preheated and highly diluted mixtures in MILD combustion lead to a relatively slow reaction time scale compared to the conventional combustion systems [27]. Despite the considerable practical applications developed in the last decades, the lack of a fundamental understanding of MILD combustion in a wide range of operating conditions somehow further limits its extensive applications at an industrial level.

Recently, Sabia et al. [27] studied ignition delay times of lean $CH_4/O_2/N_2$ mixtures in typical MILD operating conditions. These experiments extend the current database on auto-ignition times, adding useful data for lean mixtures at atmospheric pressure and moderate temperature. Methane combustion was investigated in a non-isothermal plug flow reactor (PFR) at intermediate and high temperatures. The ignition delay time was defined as the contact time required by the system to obtain a temperature increase of 10 K with respect to the inlet temperature [27,33]. The ignition delay time in this reactor is practically independent on inlet flow velocity. This fact was primarily verified by varying the inlet flow velocities in the range of 30–50 m/s.

Figure 14 shows the ignition delay times at various lean C/O ratios (0.025–0.2) with a fixed 85% N_2 dilution [27]. Two sets of ignition time relative to inflow velocity of 30 and 35 m/s for each mixture are reported and compared with model predictions. The results demonstrate a negligible effect of the inflow velocity on the measurements and predictions of ignition delay times. Considering the uncertainty of temperature measurements, as well as of the overall heat transfer coefficient, here assumed as $h = 100\,W/K/m^2$, the model predictions agree satisfactorily with the experimental data.

The auto-ignition time of the ultra-lean mixture (C/O = 0.025) is shorter than the one of other mixtures because the lower methane content reduces the extent of methyl recombination, thus promoting the oxidation pathways. This feature is entirely

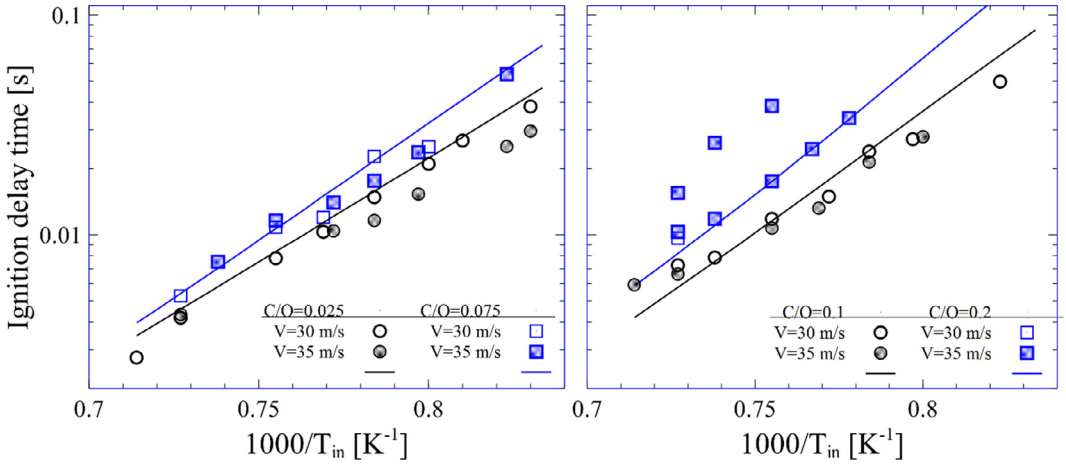

Fig. 14. Ignition delay times of four lean mixture diluted with 85% N_2 and two different inlet velocity (30 and 35 m/s). Symbols refer to experiments [27], and lines show the model predictions at 30 and 35 m/s.

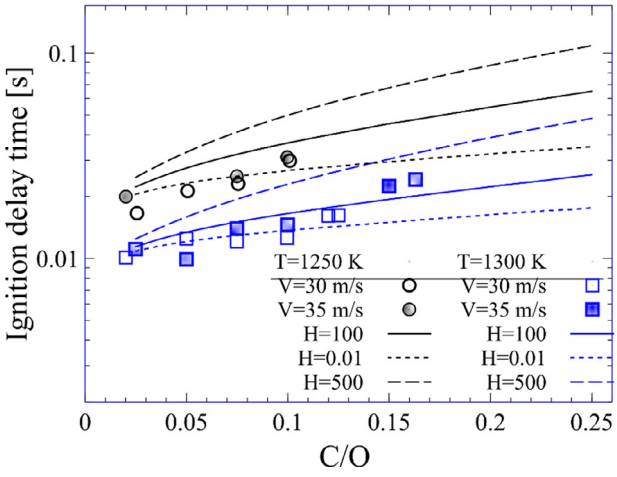

Fig. 15. Ignition delay time versus C/O ratio at 1250 and 1300 K diluted in 85% nitrogen and two different inlet velocity (30 and 35 m/s). Symbols refer to experiments [3], and the lines show the model predictions. $h = 100$ (w/K/m^2) refers to predictions with the expected global heat transfer coefficient, whereas $h = 0.01$ and $h = 500$ (w/K/m^2) refer to near adiabatic and near isothermal conditions, respectively.

consistent with the empirical expression of methane ignition delay times, which depends typically on methane concentration to a power 0.3–0.5, usually derived at higher equivalence ratios [95,99].

The model accurately predicts also the apparent activation energy, which spans between 35,000 and 42,000 cal/mol, depending on the different cases. As clearly discussed by Sabia et al. [27], a transitional regime with two auto-ignition times was detected in the experiments for the near stoichiometric mixture (C/O = 0.2). This fact can explain the more substantial discrepancies observed in Fig. 14. It is clear that at high temperatures and higher methane concentration, the assumption of an ideal plug flow reactor, without significant material and thermal axial diffusion terms is no longer correct. Thus, the observed presence of hysteresis effects and multiple steady-state solutions [100] are due to the reaction heat and the relevant interactions between the thermal feedback and the overall heat transfer. In these conditions, the accurate description of the reactor becomes more critical than the identification and validation of the kinetic mechanism, and this aspect goes beyond the scope of this work.

The facility effects on the ignition delay time for these data [27] is further analysed in Fig. 15 where the ignition delay times versus C/O ratio are reported at 1250 and 1300 K. Three sets of simulations are presented, differing for the global heat transfer coefficient. Together with the model prediction obtained by assuming $h = 100$ W/m^2 K (as reported in the paper), a nearly-adiabatic (0.01 W/m^2 K) and nearly-isothermal (500 W/m^2 K) simulation are also reported. It is worth highlighting that the variation of the heat transfer coefficient significantly affects the ignition delay time, mainly at high C/O values. On the contrary, this effect is negligible for the ultra-lean system (C/O = 0.025), where the total reaction heat is minimal. The most striking observation emerging herein is that the heat exchange largely influences these experimental data.

6. Conclusion

This study collects experimental data of relevance for MILD and OXY-fuel combustion of methane that have been reported in recent years. Such a large number of data has been analysed by means of a detailed kinetic mechanism and exhibited good predictive capabilities. Therefore, it can provide a robust starting point for detailed insights encouraging further refinement of peculiar kinetic aspects and further experimental investigations of MILD and OXY-fuel combustion. Moreover, this validated model provides a solid basis for use in benchmarking large scale modelling with facility-level experiments after appropriate reduction.

The detailed kinetic mechanism successfully captures the effect of various bath gases in MILD and OXY-fuel combustion over a broad range of conditions. Sensitivity and reactive path analyses clearly highlight the dominant kinetics. A particular focus has been devoted to assessing the relative contributions of the physical and chemical effect of the diluents on the reactivity. Laminar flame speeds, ignition delay times, and formation of products are strongly dependent on the operating conditions (temperature, pressure, and equivalence ratios), making the role of bath gases largely case sensitive. For example, at high temperature or low pressures, third body reactions are of lower importance. However, third body reactions may correspond to propagation steps, which form radicals with lower reactivity (e.g. $H + O_2(+M) = HO_2(+M)$) enhancing recombination reactions in the system. An additional example can be the removal of reactive H radicals from flames (e.g. $H + CH_3(+M) = CH_4(+M)$), or initiation reactions triggering reactivity in the transition from intermediate ($1000 < T < 1200$ K) to high temperatures ($T > 1200$ K), such as $H_2O_2(+M) = OH + OH(+M)$.

From the kinetic analysis presented in this paper, the following main features can be summarised. All of these features are correctly captured by the kinetic model attached to this study.

- H_2O and CO_2 dilution reduce the system reactivity. The effect of H_2O is more relevant than CO_2, mostly due to chemical effects related to enhanced third body collisional efficiencies that favour chain termination over branching pathways, at the operating conditions of JSR experiments. Additionally, it is highlighted that the inhibition effect vanishes for increasing pressure, as expected because of the rate constant is gradually approaching the high-pressure limit.
- The chemical effect of water gradually vanishes at high temperatures (1300–1400 K) in the flow reactor. This behaviour is due to the transition to the hot ignition regime, occurring according to the sequence $HO_2 \leftrightarrow H_2O_2 \leftrightarrow OH + OH$.
- H_2O and CO_2 additions greatly reduce laminar flame speeds, and here the CO_2 effect is more relevant. This effect is mostly related to thermal effects in the case of water, and a combination of thermal and radical scavenging effects in the case of CO_2. For these reasons, CO_2 has the highest impact on inhibiting flame propagation.
- At high-temperature conditions, the effect of CO_2 addition on methane ignition delay times is very marginal as its stability does not allow to affect ignition chemistry. This is justified by the broader temperature range involved in the propagation of a laminar flame, concerning shock tubes ignition measurements, where the reactivity is mainly sensitive to the reflected shock conditions.
- Despite the satisfactory agreement, model predictions in the case of water dilution could benefit from a more fundamental evaluation of collisional efficiency compared to the current value, usually ranging between 6 and 12. However, recent research efforts are devoted to better a priori assessment of energy-transferring collisions and pressure-dependent kinetics based on master equation simulations. A better description of relevant reactions proceeding through the formation of rovibrationally excited complexes will also benefit from the implementation of non-linear mixture rules.

Declaration of Competing Interest

None

Acknowledgments

This project has received funding from the European Union's Horizon 2020 research and innovation programme under the Marie Sklodowska-Curie grant agreement No 643134.

Supplementary materials

Supplementary material associated with this article can be found, in the online version, at doi:10.1016/j.combustflame.2019.10.014.

References

[1] S.M. Burke, U. Burke, R. Mc Donagh, O. Mathieu, I. Osorio, C. Keesee, A. Morones, E.L. Petersen, W. Wang, T.A. DeVerter, M.A. Oehlschlaeger, B. Rhodes, R.K. Hanson, D.F. Davidson, B.W. Weber, C.-J. Sung, J. Santner, Y. Ju, F.M. Haas, F.L. Dryer, E.N. Volkov, E.J.K. Nilsson, A.A. Konnov, M. Alrefae, F. Khaled, A. Farooq, P. Dirrenberger, P.-A. Glaude, F. Battin-Leclerc, H.J. Curran, An experimental and modeling study of propene oxidation. part 2: ignition delay time and flame speed measurements, Combust. Flame 162 (2015) 296–314, doi:10.1016/j.combustflame.2014.07.032.

[2] D.A. Vallero, Environmental impacts of energy production, distribution and transport, Future Energy, Elsevier, 2014, pp. 551–581, doi:10.1016/B978-0-08-099424-6.00025-9.

[3] Paris Agreement, United Nations Framework Convention on Climate Change, Paris (2016).

[4] International Energy Agency, World Energy Outlook 2018, 2018. https://www.iea.org/weo2018/scenarios/.

[5] C.K. Westbrook, F.L. Dryer, Chemical kinetic modeling of hydrocarbon combustion, Prog. Energy Combust. Sci. 10 (1984) 1–57, doi:10.1016/0360-1285(84)90118-7.

[6] A. Cavaliere, M. de Joannon, Mild combustion, Prog. Energy Combust. Sci. 30 (2004) 329–366, doi:10.1016/j.pecs.2004.02.003.

[7] A.A.V. Perpignan, A. Gangoli Rao, D.J.E.M. Roekaerts, Flameless combustion and its potential towards gas turbines, Prog. Energy Combust. Sci. 69 (2018) 28–62, doi:10.1016/J.PECS.2018.06.002.

[8] J. Wünning, Flameless oxidation to reduce thermal no-formation, Prog. Energy Combust. Sci. 23 (1997) 81–94, doi:10.1016/S0360-1285(97)00006-3.

[9] T. Hasegawa, S. Mochida, A.K. Gupta, Development of advanced industrial furnace using highly preheated combustion air, J. Propuls. Power. 18 (2002) 233–239, doi:10.2514/2.5943.

[10] N. Peters, Principles and potential of hicot combustion, Proceedings of the Forum on High Temperature Air Combustion Technology (2001), p. 109.

[11] A.E.E. Khalil, A.K. Gupta, Towards colorless distributed combustion regime, Fuel 195 (2017) 113–122, doi:10.1016/J.FUEL.2016.12.093.

[12] S. Imtenan, M. Varman, H.H. Masjuki, M.A. Kalam, H. Sajjad, M.I. Arbab, I.M. Rizwanul Fattah, Impact of low temperature combustion attaining strategies on diesel engine emissions for diesel and biodiesels: a review, Energy Convers. Manag. 80 (2014) 329–356, doi:10.1016/J.ENCONMAN.2014.01.020.

[13] D. Dunn-Rankin, Lean combustion: technology and control, Academic Press, 2011.

[14] B. Anthony, A. Hoteit, Overview of oxy-combustion technologies with pure oxygen and chemical looping combustion, Handbook of Combustion, Wiley-VCH Verlag GmbH & Co. KGaA, Weinheim, Germany, 2010, doi:10.1002/9783527628148.hoc090.

[15] R. Lückerath, W. Meier, M. Aigner, FLOX ® combustion at high pressure with different fuel compositions, J. Eng. Gas Turbines Power 130 (2008), doi:10.1115/1.2749280.

[16] C. Duwig, D. Stankovic, L. Fuchs, G. Li, E. Gutmark, Experimental and numerical study of flameless combustion in a model gas turbine combustor, Combust. Sci. Technol. 180 (2008) 279–295, doi:10.1080/00102200701739164.

[17] H. Schütz, O. Lammel, G. Schmitz, T. Rödiger, M. Aigner, EZEE®: a high power density modulating FLOX® combustor, Proceedings of the ASME Turbo Expo (2012), pp. 701–712, doi:10.1115/GT2012-68997.

[18] A.S. Veríssimo, A.M.A. Rocha, M. Costa, Experimental study on the influence of the thermal input on the reaction zone under flameless oxidation conditions, Fuel Process. Technol. 106 (2013) 423–428, doi:10.1016/j.fuproc.2012.09.008.

[19] A.S. Veríssimo, A.M.A. Rocha, M. Costa, Importance of the inlet air velocity on the establishment of flameless combustion in a laboratory combustor, Exp. Therm. Fluid Sci. 44 (2013) 75–81, doi:10.1016/j.expthermflusci.2012.05.015.

[20] Y. Levy, V. Sherbaum, V. Erenburg, The role of the recirculating gases at the mild combustion regime formation, Vol. 2 Turbo Expo 2007, ASME (2007), pp. 271–278, doi:10.1115/GT2007-27369.

[21] M.J. Melo, J.M.M. Sousa, M. Costa, Y. Levy, Flow and combustion characteristics of a low-NOx combustor model for gas turbines, J. Propuls. Power. 27 (2011) 1212–1217, doi:10.2514/1.B34033.

[22] B.B. Dally, A.N. Karpetis, R.S. Barlow, Structure of turbulent non-premixed jet flames in a diluted hot coflow, Proc. Combust. Inst. 29 (2002) 1147–1154, doi:10.1016/S1540-7489(02)80145-6.

[23] R.W. Bilger, S.B. Pope, K.N.C. Bray, J.F. Driscoll, Paradigms in turbulent combustion research, Proc. Combust. Inst. 30 (2005) 21–42, doi:10.1016/j.proci.2004.08.273.

[24] M. Lubrano Lavadera, P. Sabia, G. Sorrentino, R. Ragucci, M. de Joannon, Experimental study of the effect of CO_2 on propane oxidation in a jet stirred flow reactor, Fuel 184 (2016) 876–888, doi:10.1016/j.fuel.2016.06.046.

[25] M. De Joannon, P. Sabia, A. Tregrossi, A. Cavaliere, DILUTION effects in natural gas mild combustion, Clean Air Int. J. Energy Clean Environ 7 (2006) 127–139, doi:10.1615/InterJEnerCleanEnv.v7.i2.30.

[26] G. Bagheri, M.L. Lavadera, E. Ranzi, M. Pelucchi, P. Sabia, M. de Joannon, A. Parente, T. Faravelli, Thermochemical oscillation of methane mild combustion diluted with $N_2/CO_2/H_2O$, Combust. Sci. Technol. 191 (2019) 68–80, doi:10.1080/00102202.2018.1452411.

[27] P. Sabia, M. de Joannon, A. Picarelli, R. Ragucci, Methane auto-ignition delay times and oxidation regimes in mild combustion at atmospheric pressure, Combust. Flame 160 (2013) 47–55, doi:10.1016/j.combustflame.2012.09.015.

[28] R. Weber, J.P. Smart, W. Vd Kamp, On the (MILD) combustion of gaseous, liquid, and solid fuels in high temperature preheated air, Proc. Combust. Inst. 30 (2005) 2623–2629, doi:10.1016/j.proci.2004.08.101.

[29] P. Li, B.B. Dally, J. Mi, F. Wang, MILD oxy-combustion of gaseous fuels in a laboratory-scale furnace, Combust. Flame 160 (2013) 933–946, doi:10.1016/j.combustflame.2013.01.024.

[30] M. de Joannon, P. Sabia, A. Tregrossi, A. Cavaliere, Dynamic behavior of methane oxidation in premixed flow reactor, Combust. Sci. Technol. 176 (2004) 769–783, doi:10.1080/00102200490428387.

[31] P. Sabia, M. de Joannon, S. Fierro, A. Tregrossi, A. Cavaliere, Hydrogen-enriched methane mild combustion in a well stirred reactor, Exp. Therm. Fluid Sci. 31 (2007) 469–475, doi:10.1016/j.expthermflusci.2006.04.016.

[32] F. Wang, P. Li, Z. Mei, J. Zhang, J. Mi, Combustion of $CH_4/O_2/N_2$ in a well stirred reactor, Energy 72 (2014) 242–253, doi:10.1016/j.energy.2014.05.029.

[33] P. Sabia, M. Lubrano Lavadera, G. Sorrentino, P. Giudicianni, R. Ragucci, M. De Joannon, H_2O and CO_2 dilution in mild combustion of simple hydrocarbons, Flow, Turbul. Combust. 96 (2016) 433–448, doi:10.1007/s10494-015-9667-4.

[34] F. Wang, J. Mi, P. Li, Combustion regimes of a jet diffusion flame in hot coflow, Energy Fuels 27 (2013) 3488–3498, doi:10.1021/ef400500w.

[35] P.R. Medwell, M.J. Evans, Q.N. Chan, V.R. Katta, Laminar flame calculations for analyzing trends in autoignitive jet flames in a hot and vitiated coflow, Energy Fuels 30 (2016) 8680–8690, doi:10.1021/acs.energyfuels.6b01264.

[36] M.J. Evans, P.R. Medwell, H. Wu, A. Stagni, M. Ihme, Classification and lift-off height prediction of non-premixed mild and autoignitive flames, Proc. Combust. Inst. 36 (2017) 4297–4304, doi:10.1016/J.PROCI.2016.06.013.

[37] P. Li, J. Mi, B.B. Dally, F. Wang, L. Wang, Z. Liu, S. Chen, C. Zheng, Progress and recent trend in mild combustion, Sci. China Technol. Sci. 54 (2011) 255–269, doi:10.1007/s11431-010-4257-0.

[38] B. Danon, A. Swiderski, W. de Jong, W. Yang, D.J.E.M. Roekaerts, Emission and efficiency comparison of different firing modes in a furnace with four hitac burners, Combust. Sci. Technol. 183 (2011) 686–703, doi:10.1080/00102202.2011.553643.

[39] M. Oberlack, R. Arlitt, N. Peters, On stochastic damköhler number variations in a homogeneous flow reactor, Combust. Theory Model. 4 (2000) 495–509, doi:10.1088/1364-7830/4/4/307.

[40] M. de Joannon, P. Sabia, A. Cavaliere, MILD combustion, Handbook on combustion, Wiley-VCH Verlag GmbH & Co. KGaA, Weinheim, Germany, 2010, pp. 237–256, doi:10.1002/9783527628148.hoc081.

[41] A.A. Konnov, M.T. Javed, H. Kassman, N. Irfan, NOx formation, control and reduction techniques, Handbook on combustion, Wiley-VCH Verlag GmbH & Co. KGaA, 2010, doi:10.1002/9783527628148.hoc037.

[42] M.A. Galbiati, A. Cavigiolo, A. Effuggi, D. Gelosa, R. Rota, MILD combustion for fuel-no x reduction, Combust. Sci. Technol. 176 (2004) 1035–1054, doi:10.1080/00102200490426424.

[43] K.W. Lee, D.H. Choi, Analysis of no formation in high temperature diluted air combustion in a coaxial jet flame using an unsteady flamelet model, Int. J. Heat Mass Transf. 52 (2009) 1412–1420, doi:10.1016/j.ijheatmasstransfer.2008.08.015.

[44] M. Abian, M.U. Alzueta, P. Glarborg, Formation of no from N_2/O_2 mixtures in a flow reactor: toward an accurate prediction of thermal no, Int. J. Chem. Kinet. 47 (2015) 518–532, doi:10.1002/kin.20929.

[45] I. Glassman, R.A. Yetter, N.G. Glumac, Combustion, Elsevier, 2015, doi:10.1016/C2011-0-05402-9.

[46] R. Stanger, T. Wall, R. Spörl, M. Paneru, S. Grathwohl, M. Weidmann, G. Scheffknecht, D. McDonald, K. Myöhänen, J. Ritvanen, S. Rahiala, T. Hyppänen, J. Mletzko, A. Kather, S. Santos, Oxyfuel combustion for CO_2 capture in power plants, Int. J. Greenh. Gas Control 40 (2015) 55–125, doi:10.1016/J.IJGGC.2015.06.010.

[47] L. Chen, S.Z. Yong, A.F. Ghoniem, Oxy-fuel combustion of pulverized coal: characterization, fundamentals, stabilization and cfd modeling, Prog. Energy Combust. Sci. 38 (2012) 156–214, doi:10.1016/J.PECS.2011.09.003.

[48] C.E. Baukal, Oxygen-enhanced combustion, CRC Press, 2013 https://www.crcpress.com/Oxygen-Enhanced-Combustion/Jr/p/book/9781439862285 (accessed June 28, 2019).

[49] W.K. Metcalfe, S.M. Burke, S.S. Ahmed, H.J. Curran, A hierarchical and comparative kinetic modeling study of C1 - C2 hydrocarbon and oxygenated fuels, Int. J. Chem. Kinet 45 (2013) 638–675, doi:10.1002/kin.20802.

[50] E. Ranzi, A. Frassoldati, R. Grana, A. Cuoci, T. Faravelli, A.P. Kelley, C.K. Law, Hierarchical and comparative kinetic modeling of laminar flame speeds of hy-

drocarbon and oxygenated fuels, Prog. Energy Combust. Sci. 38 (2012) 468–501, doi:10.1016/j.pecs.2012.03.004.
[51] E. Ranzi, A. Frassoldati, A. Stagni, M. Pelucchi, A. Cuoci, T. Faravelli, Reduced kinetic schemes of complex reaction systems: fossil and biomass-derived transportation fuels, Int. J. Chem. Kinet. 46 (2014) 512–542, doi:10.1002/kin.20867.
[52] M. Pelucchi, E. Ranzi, A. Frassoldati, T. Faravelli, Alkyl radicals rule the low temperature oxidation of long chain aldehydes, Proc. Combust. Inst. (2016) 000 doi: http://dx.doi.org/10.1016/j.proci.2016.05.051 .
[53] E.L. Ranzi, M. Dente, T. Faravelli, G. Pennati, Prediction of kinetic parameters for hydrogen abstraction reactions, Combust. Sci. Technol. 95 (1993) 1–50, doi:10.1080/00102209408935325.
[54] B. Ruscic, R.E. Pinzon, G. Von Laszewski, D. Kodeboyina, A. Burcat, D. Leahy, D. Montoy, A.F. Wagner, Active thermochemical tables: thermochemistry for the 21st century, J. Phys. Conf. Ser. 16 (2005) 561–570, doi:10.1088/1742-6596/16/1/078.
[55] A. Burcat, B. Ruscic, Third millennium ideal gas and condensed phase thermochemical database for combustion with updates from active thermochemical tables, Tech. Rep. ANL-05/20 (2005) ANL-05/20 TAE 960. doi:10.2172/925269.
[56] W. Tsang, R.F. Hampson, Chemical kinetic data base for combustion chemistry. part 1. methane and related compounds, J. Phys. Chem. Ref. Data. 15 (1986) 1087–1279, doi:10.1063/1.555759.
[57] N. Hansen, J.A. Miller, P.R. Westmoreland, T. Kasper, K. Kohse-Höinghaus, J. Wang, T.A. Cool, Isomer-specific combustion chemistry in allene and propyne flames, Combust. Flame 156 (2009) 2153–2164, doi:10.1016/J.COMBUSTFLAME.2009.07.014.
[58] G.P. Smith, D.M. Golden, M. Frenklach, N.W. Moriarty, B. Eiteneer, M. Goldenberg, C.T. Bowman, R.K. Hanson, S. Song, W.C. Gardiner Jr., V.V. Lissianski, Z. Qin, GRI-Mech 3.0, 1999, URL Http// Www.Me.Berkeley.Edu/Gri_mech/ . (n.d.).
[59] Z. Hong, D.F. Davidson, E.A. Barbour, R.K. Hanson, A new shock tube study of the $H+O_2 \rightarrow OH+O$ reaction rate using tunable diode laser absorption of H_2O near 2.5 μm, Proc. Combust. Inst. 33 (2011) 309–316, doi:10.1016/j.proci.2010.05.101.
[60] J. Lee, C.-J. Chen, J.W. Bozzelli, Thermochemical and kinetic analysis of the acetyl radical (CH_3 C • O) + O_2 reaction system, J. Phys. Chem. A 106 (2002) 7155–7170, doi:10.1021/jp014443g.
[61] S.G. Davis, C.K. Law, H. Wang, Propyne pyrolysis in a flow reactor: an experimental, RRKM, and detailed kinetic modeling study, J. Phys. Chem. A 103 (1999) 5889–5899, doi:10.1021/jp982762a.
[62] C. Cavallotti, M. Pelucchi, Y. Georgievskii, S.J. Klippenstein, EStokTP: electronic structure to temperature- and pressure-dependent rate constants-a code for automatically predicting the thermal kinetics of reactions, J. Chem. Theory Comput. 15 (2019) 1122–1145, doi:10.1021/acs.jctc.8b00701.
[63] J.A. Miller, S.J. Klippenstein, From the multiple-well master equation to phenomenological rate coefficients: reactions on a c 3 h 4 potential energy surface, J. Phys. Chem. A. 107 (2003) 2680–2692, doi:10.1021/jp0221082.
[64] L.B. Harding, S.J. Klippenstein, Y. Georgievskii, On the combination reactions of hydrogen atoms with resonance-stabilized hydrocarbon radicals †, J. Phys. Chem. A 111 (2007) 3789–3801, doi:10.1021/jp0682309.
[65] J.A. Miller, J.P. Senosiain, S.J. Klippenstein, Y. Georgievskii, Reactions over multiple, interconnected potential wells: unimolecular and bimolecular reactions on a c 3 h 5 potential †, J. Phys. Chem. A. 112 (2008) 9429–9438, doi:10.1021/jp804510k.
[66] A. Cuoci, A. Frassoldati, T. Faravelli, E. Ranzi, OpenSMOKE++: an object-oriented framework for the numerical modeling of reactive systems with detailed kinetic mechanisms, Comput. Phys. Commun. 192 (2015) 237–264, doi:10.1016/j.cpc.2015.02.014.
[67] S. Turns, An introduction to combustion: concepts and applications, 3rd ed, McGraw-hill, New York, 2012.
[68] T. Plessing, N. Peters, J.G. Wünning, Laseroptical investigation of highly preheated combustion with strong exhaust gas recirculation, Symp. Combust. 27 (1998) 3197–3204, doi:10.1016/S0082-0784(98)80183-5.
[69] Z. Chen, V.M. Reddy, S. Ruan, N.A.K. Doan, W.L. Roberts, N. Swaminathan, Simulation of mild combustion using perfectly stirred reactor model, Proc. Combust. Inst. 36 (2015) 4279–4286, doi:10.1016/j.proci.2016.06.007.
[70] M. de Joannon, G. Sorrentino, A. Cavaliere, MILD combustion in diffusion-controlled regimes of hot diluted fuel, Combust. Flame 159 (2012) 1832–1839, doi:10.1016/J.COMBUSTFLAME.2012.01.013.
[71] M. de Joannon, A. Cavaliere, T. Faravelli, E. Ranzi, P. Sabia, A. Tregrossi, Analysis of process parameters for steady operations in methane mild combustion technology, Proc. Combust. Inst. 30 II (2005) 2605–2612, doi:10.1016/j.proci.2004.08.190.
[72] M. Lubrano Lavadera, Y. Song, P. Sabia, O. Herbinet, M. Pelucchi, A. Stagni, T. Faravelli, F. Battin-Leclerc, M. de Joannon, Oscillatory behavior in methane combustion: influence of the operating parameters, Energy Fuels 32 (2018) 10088–10099, doi:10.1021/acs.energyfuels.8b00967.
[73] S.M. Burke, W. Metcalfe, O. Herbinet, F. Battin-Leclerc, F.M. Haas, J. Santner, F.L. Dryer, H.J. Curran, An experimental and modeling study of propene oxidation. part 1: speciation measurements in jet-stirred and flow reactors, Combust. Flame 161 (2014) 2765–2784, doi:10.1016/j.combustflame.2014.05.010.
[74] T. Kovács, I.G. Zsély, Á. Kramarics, T. Turányi, Kinetic analysis of mechanisms of complex pyrolytic reactions, J. Anal. Appl. Pyrolysis 79 (2007) 252–258, doi:10.1016/j.jaap.2006.09.007.
[75] G. Fau, N. Gascoin, P. Gillard, J. Steelant, Methane pyrolysis: literature survey and comparisons of available data for use in numerical simulations, J. Anal. Appl. Pyrolysis 104 (2013) 1–9, doi:10.1016/j.jaap.2013.04.006.
[76] O. Olsvik, F. Billaud, Modelling of the decomposition of methane at 1273K in a plug flow reactor at low conversion, J. Anal. Appl. Pyrolysis 25 (1993) 395–405, doi:10.1016/0165-2370(93)80058-8.
[77] O.A. Rokstad, O. Olsvik, A. Holmen, Thermal coupling of methane„ Nat. Gas Convers. (1991) 533–539, doi:10.1016/S0167-2991(08)60120-2.
[78] T. Le Cong, P. Dagaut, Experimental and detailed kinetic modeling of the oxidation of methane and methane/syngas mixtures and effect of carbon dioxide addition, Combust. Sci. Technol. 180 (2008) 2046–2091, doi:10.1080/00102200802265929.
[79] T. Le Cong, P. Dagaut, Effect of water vapor on the kinetics of combustion of hydrogen and natural gas: experimental and detailed modeling study, Energy Fuels 23 (2009) 725–734, doi:10.1115/GT2008-50272.
[80] T. Le Cong, P. Dagaut, Oxidation of H2/CO2mixtures and effect of hydrogen initial concentration on the combustion of CH_4 and CH_4/CO_2 mixtures: experiments and modeling, Proc. Combust. Inst. 32 I (2009) 427–435, doi:10.1016/j.proci.2008.05.079.
[81] M.S. Skjoth-Rasmussen, P. Glarborg, M. Ostberg, J.T. Johannessen, H. Livbjerg, A.D. Jensen, T.S. Christensen, M.S. Skjøth-Rasmussen, P. Glarborg, M. Østberg, J.T. Johannessen, H. Livbjerg, A.D. Jensen, T.S. Christensen, Formation of polycyclic aromatic hydrocarbons and soot in fuel-rich oxidation of methane in a laminar flow reactor, Combust. Flame 136 (2004) 91–128, doi:10.1016/j.combustflame.2003.09.011.
[82] A.N. Mazas, D.A. Lacoste, T. Schuller, Experimental and numerical investigation on the laminar flame speed of ch, Vol. 2 Combustion, Fuels and Emissions, Parts A and B. ASME (2010), pp. 411–421, doi:10.1115/GT2010-22512.
[83] Y. Xie, J. Wang, M. Zhang, J. Gong, W. Jin, Z. Huang, Experimental and numerical study on laminar flame characteristics of methane oxy-fuel mixtures highly diluted with co 2, Energy Fuels 27 (2013) 6231–6237, doi:10.1021/ef401220h.
[84] B. Koroglu, O.M. Pryor, J. Lopez, L. Nash, S.S. Vasu, Shock tube ignition delay times and methane time-histories measurements during excess CO_2 diluted oxy-methane combustion, Combust. Flame 164 (2016) 152–163, doi:10.1016/j.combustflame.2015.11.011.
[85] J.W. Hargis, E.L. Petersen, Methane ignition in a shock tube with high levels of co 2 dilution: consideration of the reflected-shock bifurcation, Energy Fuels 29 (2015) 7712–7726, doi:10.1021/acs.energyfuels.5b01760.
[86] S.J. Klippenstein, From theoretical reaction dynamics to chemical modeling of combustion, Proc. Combust. Inst. 36 (2017) 77–111, doi:10.1016/j.proci.2016.07.100.
[87] M.B. Toftegaard, J. Brix, P.A. Jensen, P. Glarborg, A.D. Jensen, Oxy-fuel combustion of solid fuels, Prog. Energy Combust. Sci. 36 (2010) 581–625, doi:10.1016/J.PECS.2010.02.001.
[88] G.H. Abd-Alla, Using exhaust gas recirculation in internal combustion engines: a review, Energy Convers. Manag. 43 (2002) 1027–1042, doi:10.1016/S0196-8904(01)00091-7.
[89] M. Zheng, G.T. Reader, J.G. Hawley, Diesel engine exhaust gas recirculation—-a review on advanced and novel concepts, Energy Convers. Manag. 45 (2004) 883–900, doi:10.1016/S0196-8904(03)00194-8.
[90] F.B. Shareh, G. Silcox, E.G. Eddings, Calculated impacts of diluents on flame temperature, ignition delay, and flame speed of methane-oxygen mixtures at high pressure and low to moderate temperatures, Energy Fuels 32 (2018) 3891–3899, doi:10.1021/acs.energyfuels.7b02647.
[91] J. Troe, V.G. Ushakov, The dissociationrecombination reaction $CH_4(+M) \Leftrightarrow CH_3 + h\ (+M)$: a case study for unimolecular rate theory, J. Chem. Phys. 136 (2012) 1–12, doi:10.1063/1.4717706.
[92] D.M. Golden, What, methane again?!, Int. J. Chem. Kinet. 45 (2013) 213–220, doi:10.1002/kin.20758.
[93] A.W. Jasper, J.A. Miller, S.J. Klippenstein, Collision efficiency of water in the unimolecular reaction $CH_4\ (+H_2O) \leftrightarrows CH_3 + h\ (+H_2O)$: one-Dimensional and two-dimensional solutions of the low-pressure-limit master equation, J. Phys. Chem. A 117 (2013) 12243–12255, doi:10.1021/jp409086w.
[94] L. Lei, M.P. Burke, Evaluating mixture rules and combustion implications for multi-component pressure dependence of allyl + HO_2 reactions, Proc. Combust. Inst. 37 (2019) 355–362, doi:10.1016/j.proci.2018.05.023.
[95] L.J. Spadaccini, M.B. Colket, Ignition delay characteristics of methane fuels, Prog. Energy Combust. Sci. 20 (1994) 431–460, doi:10.1016/0360-1285(94)90011-6.
[96] B. Koroglu, O. Pryor, J. Lopez, L. Nash, S. Vasu, Methane ignition delay times in CO2 diluted mixtures in a shock tube, 51st AIAA/SAE/ASEE Joint Propulsion Conference, Reston, Virginia, American Institute of Aeronautics and Astronautics (2015), doi:10.2514/6.2015-4088.
[97] O. Pryor, S. Barak, J. Lopez, L. Nash, E. Ninnemann, B. Koroglu, L. Nash, S. Vasu, High pressure shock tube ignition delay time measurements during oxy-methane combustion with high levels of CO<inf>2</inf>Dilution, J. Energy Resour. Technol. Trans. ASME 139 (2017) 1–6, doi:10.1115/1.4036254.
[98] O. Pryor, S. Barak, B. Koroglu, E. Ninnemann, S.S. Vasu, Measurements and interpretation of shock tube ignition delay times in highly CO_2 diluted mixtures using multiple diagnostics, Combust. Flame 180 (2017) 63–76, doi:10.1016/j.combustflame.2017.02.020.
[99] N. Lamoureux, C.-E. Paillard, V. Vaslier, Low hydrocarbon mixtures ignition delay times investigation behind reflected shock waves, Shock Waves 11 (2002) 309–322, doi:10.1007/s001930100108.
[100] G.A. Foulds, B.F. Gray, S.A. Miller, G.S. Walker, Homogeneous gas-phase oxidation of methane using oxygen as oxidant in an annular reactor, Ind. Eng. Chem. Res. 32 (1993) 780–787, doi:10.1021/ie00017a003.